



TÉCNICO  
LISBOA

# PARTICLE ACCELERATION MECHANISMS WITHIN BLAZARS

TFPAC - Pedro Costa - 87349

Teacher: Nuno Leonardo



# OUTLINE

## POINTS FOR DISCUSSION

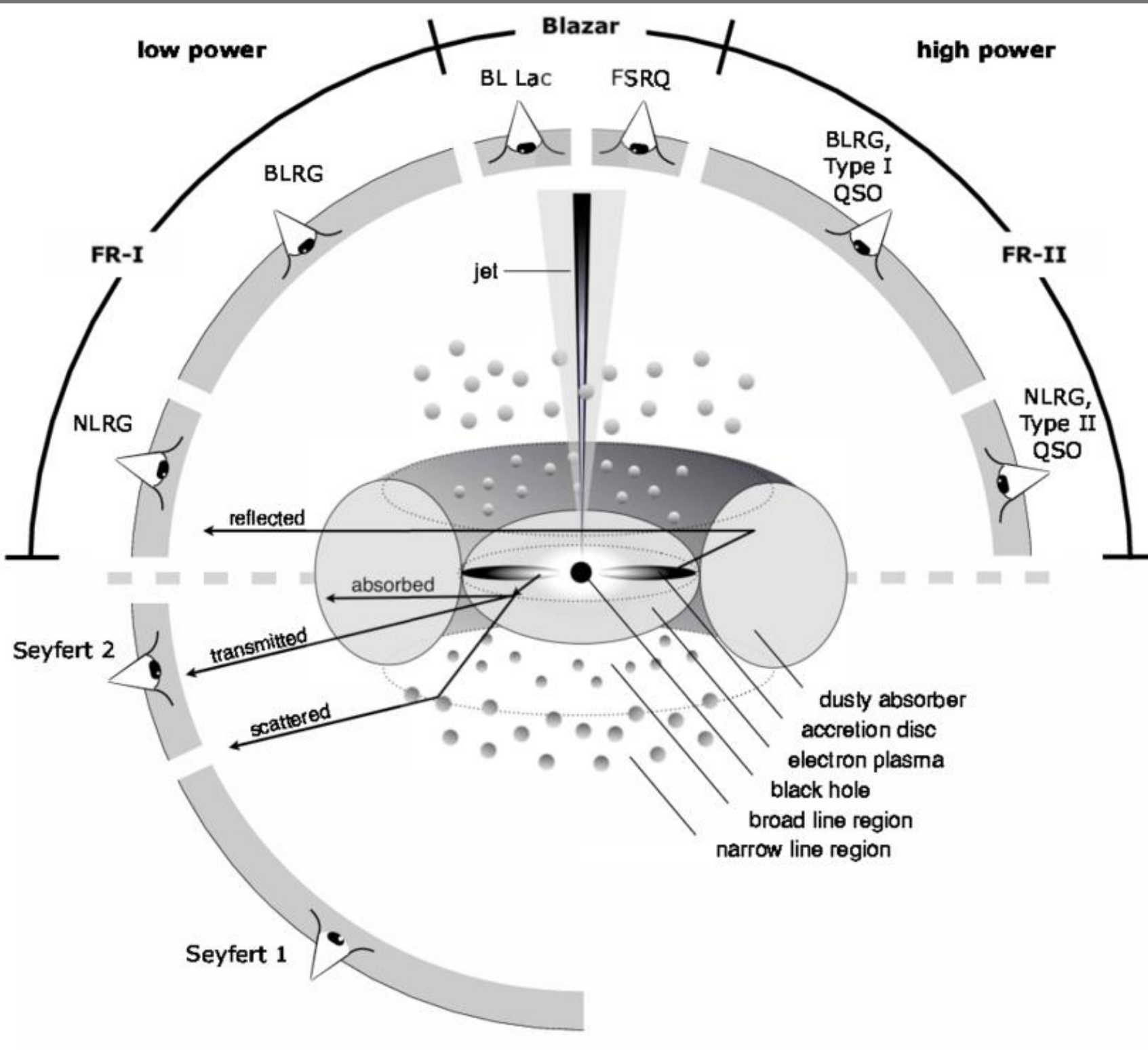
What is an AGN?

What is a blazar?

Particle Acceleration Mechanisms within blazars

The case of the TXS 0506+056 blazar and the IceCube-170922A neutrino event

Summary



## BASIC INFORMATION

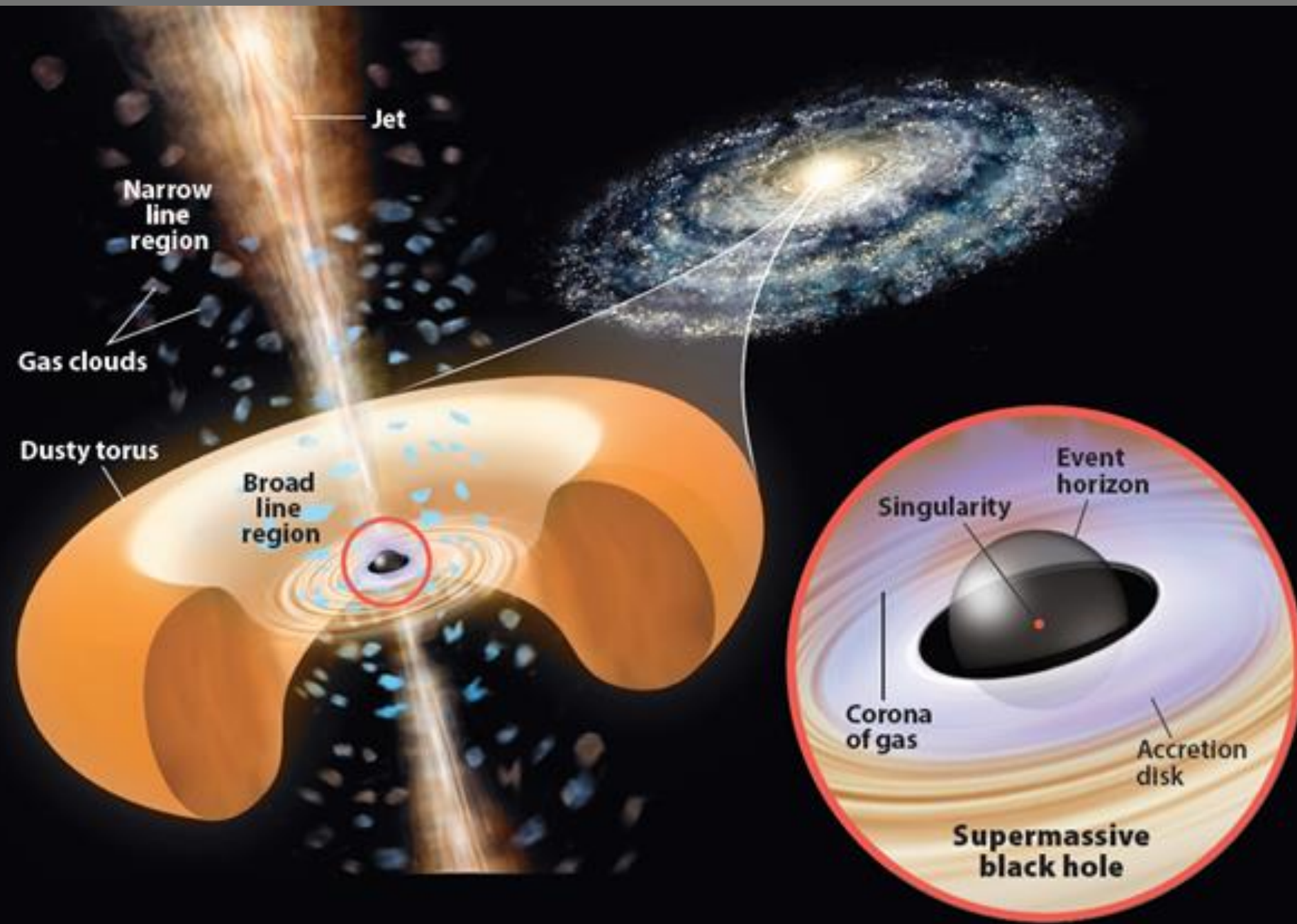
- Centre region of an active galaxy
- Very bright and compact
- Emission predominantly produced due to accretion of matter onto central black hole
- Forms an accretion disk, that heats up due to dissipation of gravitational energy into radiation,
- **Unified model:** AGN classified according to angle of observer in relation to the source

WHAT IS AN  
AGN?

# WHAT IS AN AGN?

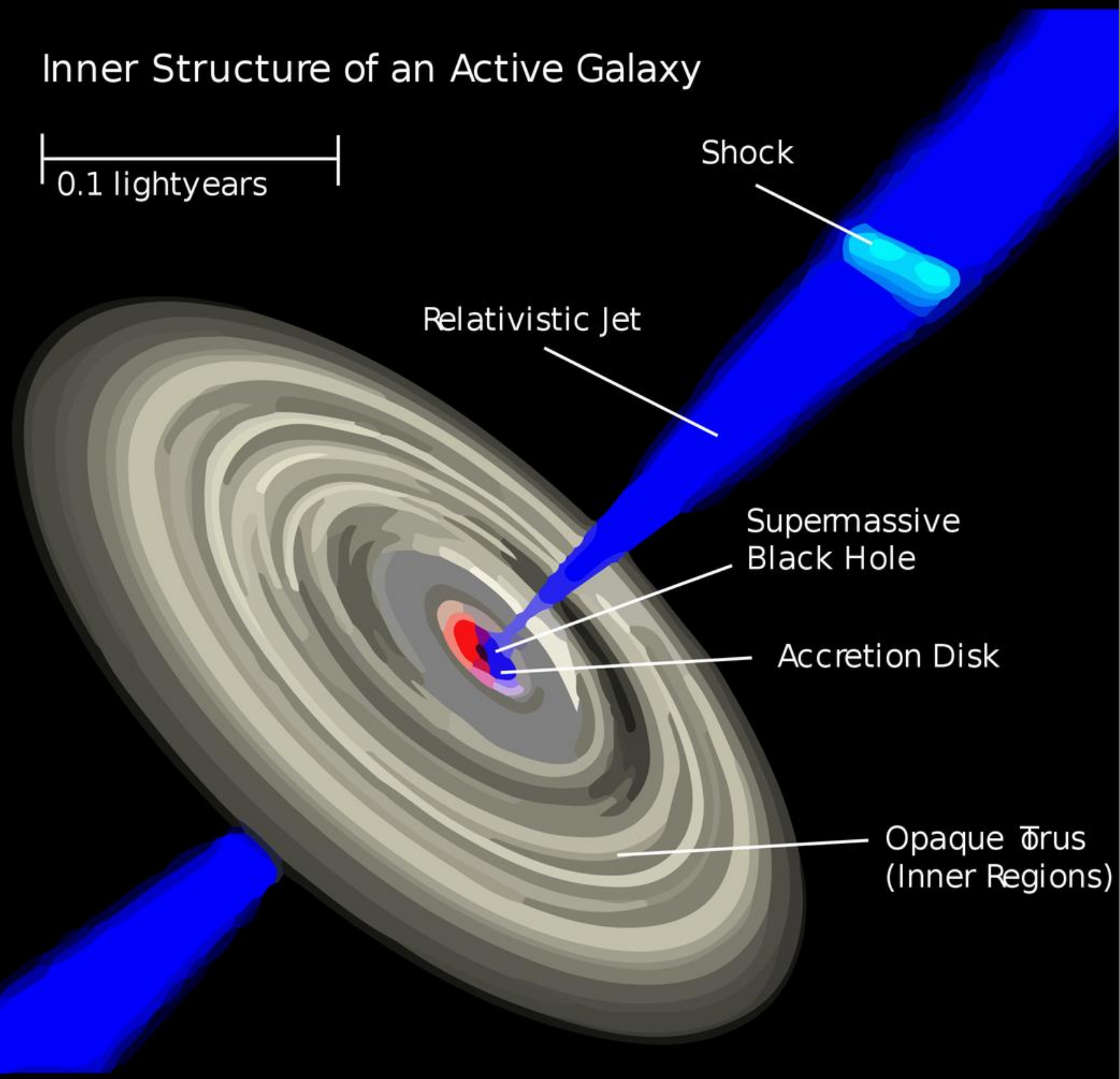
## BASIC STRUCTURE

- Centre: Supermassive black hole
- Surrounded by accretion disk
- Above disk: hot electron plasma
- Surrounded by broad line region
- Further out: torus or warped disk of gas and dust. Blocks/absorbs produced radiation



## Inner Structure of an Active Galaxy

0.1 lightyears



Particular type of AGN:

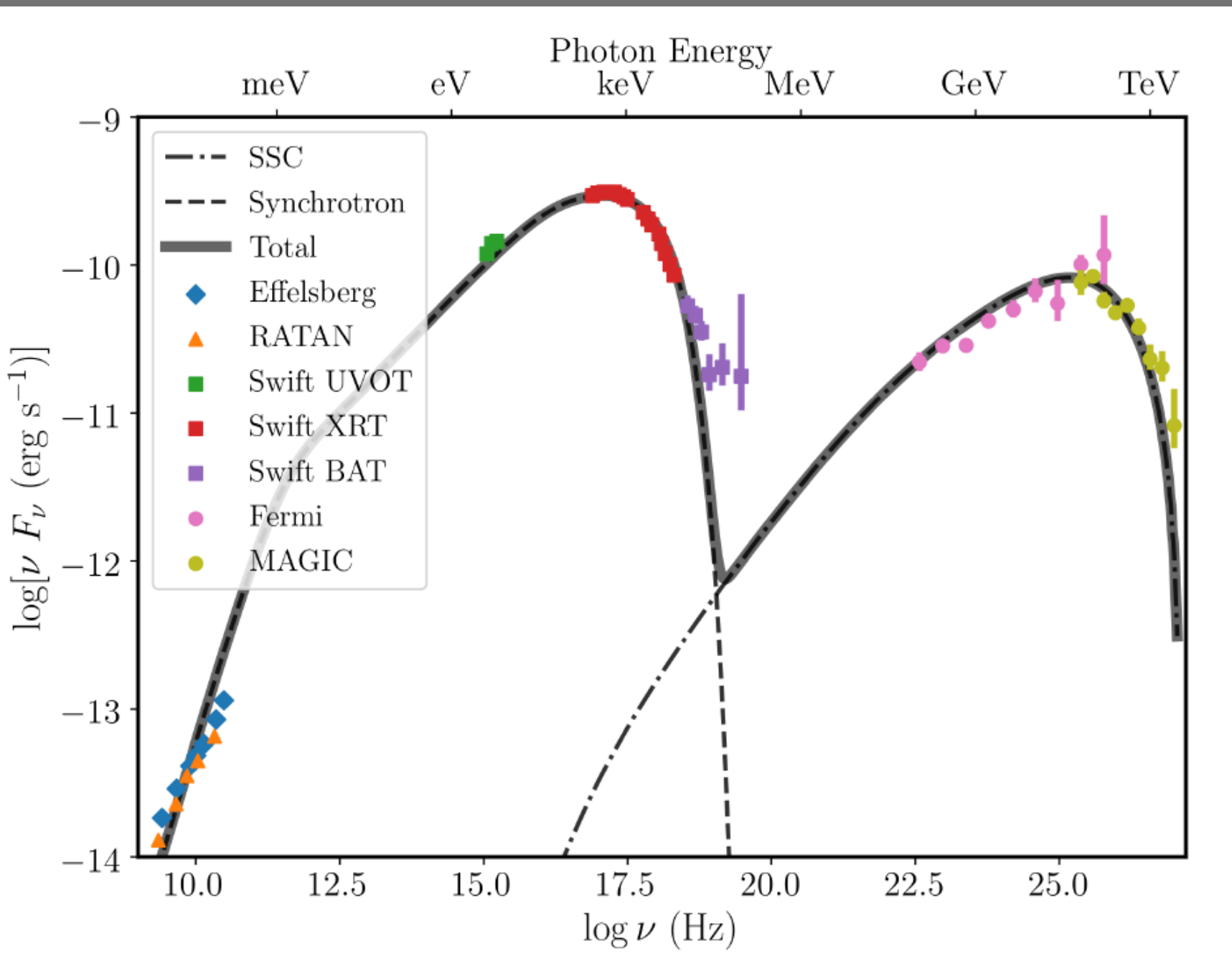
- Exhibits **relativistic jets**, directed very nearly towards observer
- Much higher luminosity
- Powerful, variable emitters from radio to gamma-ray wavelengths
- Emission and acceleration mechanisms not fully understood

# WHAT IS A BLAZAR?

# WHAT IS A BLAZZAR?

**Spectral Energy Distribution (SED)**  
exhibits characteristic 'double hump':

- Low energy peak (IR/Optical/UV/X-ray): established as synchrotron emission
- High energy peak (Gamma-rays): origin still unclear.



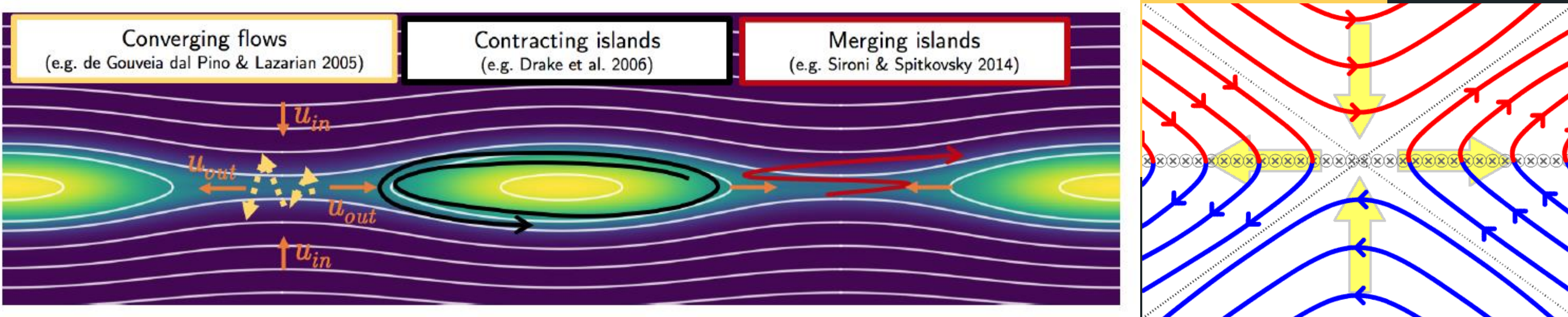
SED of the BL Lac class blazar Markarian 421

# PARTICLE ACCELERATION MECHANISMS WITHIN BLAZARS

## MAGNETIC RECONNECTION

Occurs in highly conducting plasmas. Characterised by rearrangement of magnetic field. Leads to conversion of magnetic energy to kinetic or thermal energy.

Basic concept: converging magnetic field lines approach each other and undergo resistive dissipation



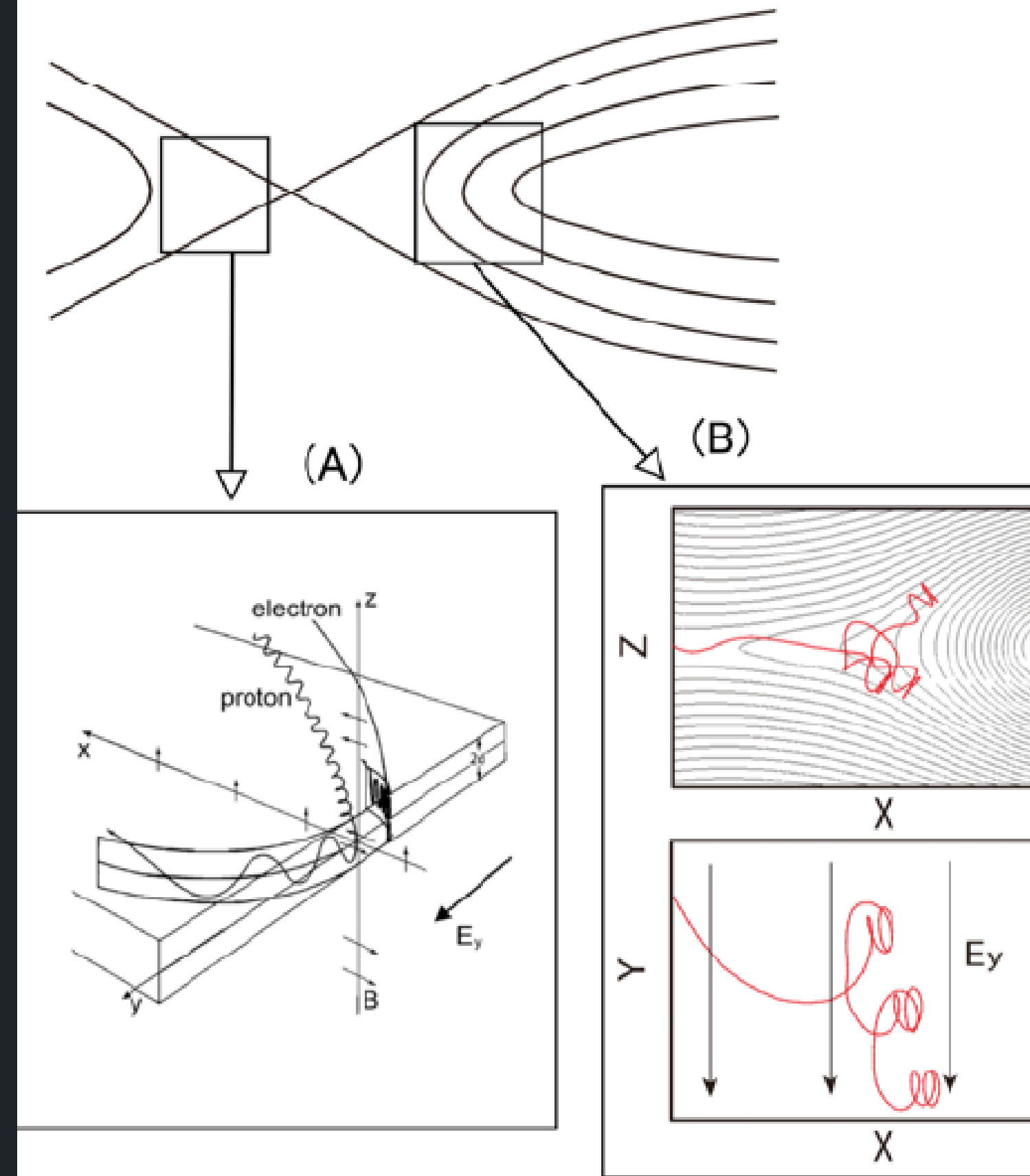
# MAGNETIC RECONNECTION

## A) SPEISER/MEANDERING MOTION

Charged particles almost directly resonate with the inductive electric field and can be quickly accelerated in the diffusion region where the magnetic field is weak

## B) GRADIENT B DRIFT IN MAGNETIC PILEUP REGION

Pileup magnetic field region produced by compression of the reconnection outflow. Curvature B drift motion for ions/electrons, which is parallel/antiparallel to the inductive electric field, contributes to the energization



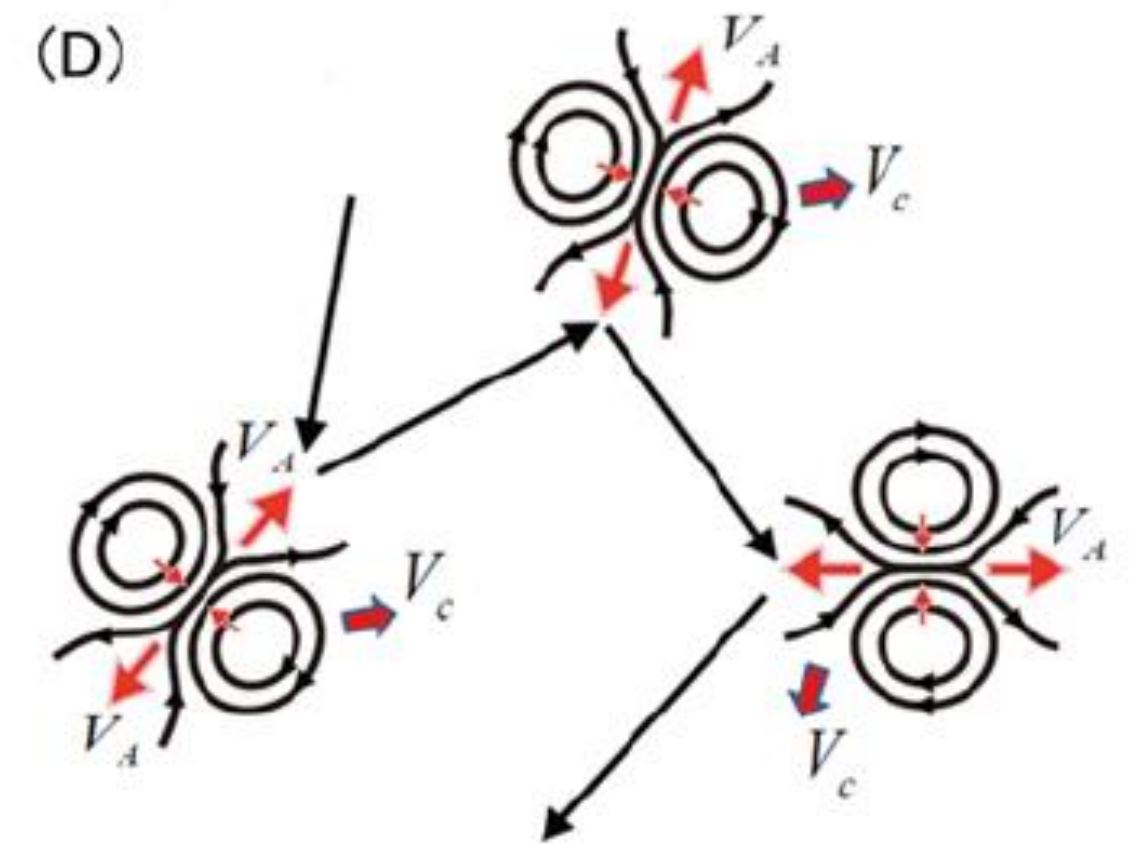
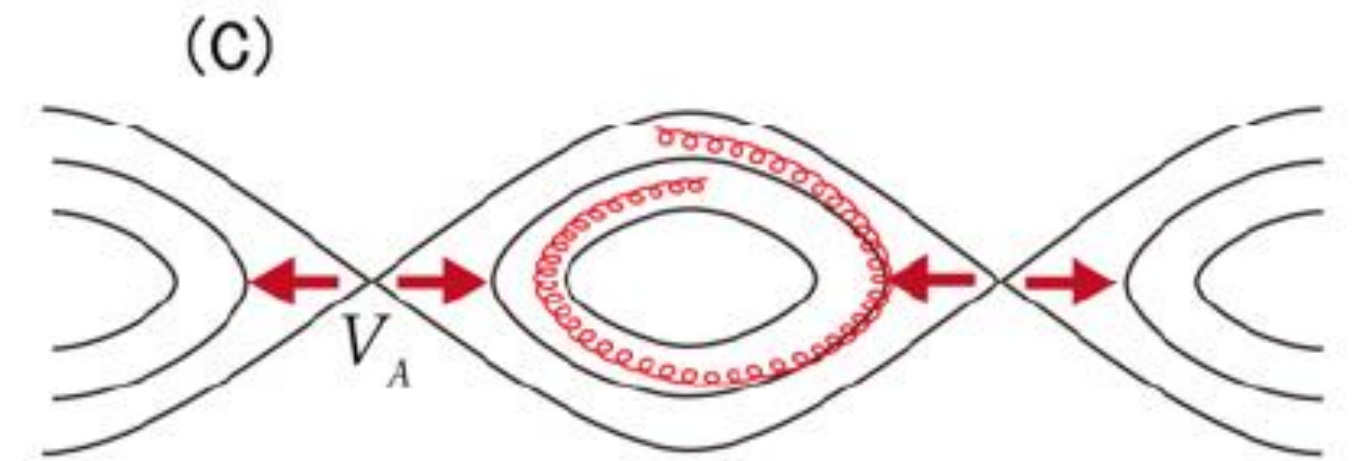
# MAGNETIC RECONNECTION

## C) ACCELERATION IN SINGLE RECONNECTION SITE

Shrinking magnetic field lines trap particles in magnetic islands. Particles can gain energy by reflection from both ends of the contracting magnetic island.

## D) 'COLLISION' WITH MULTIPLE MAGNETIC ISLANDS

Analogous to Fermi acceleration model, where particles gain energy stochastically during head-on collisions with many magnetic clouds, with magnetic clouds being replaced by magnetic islands.

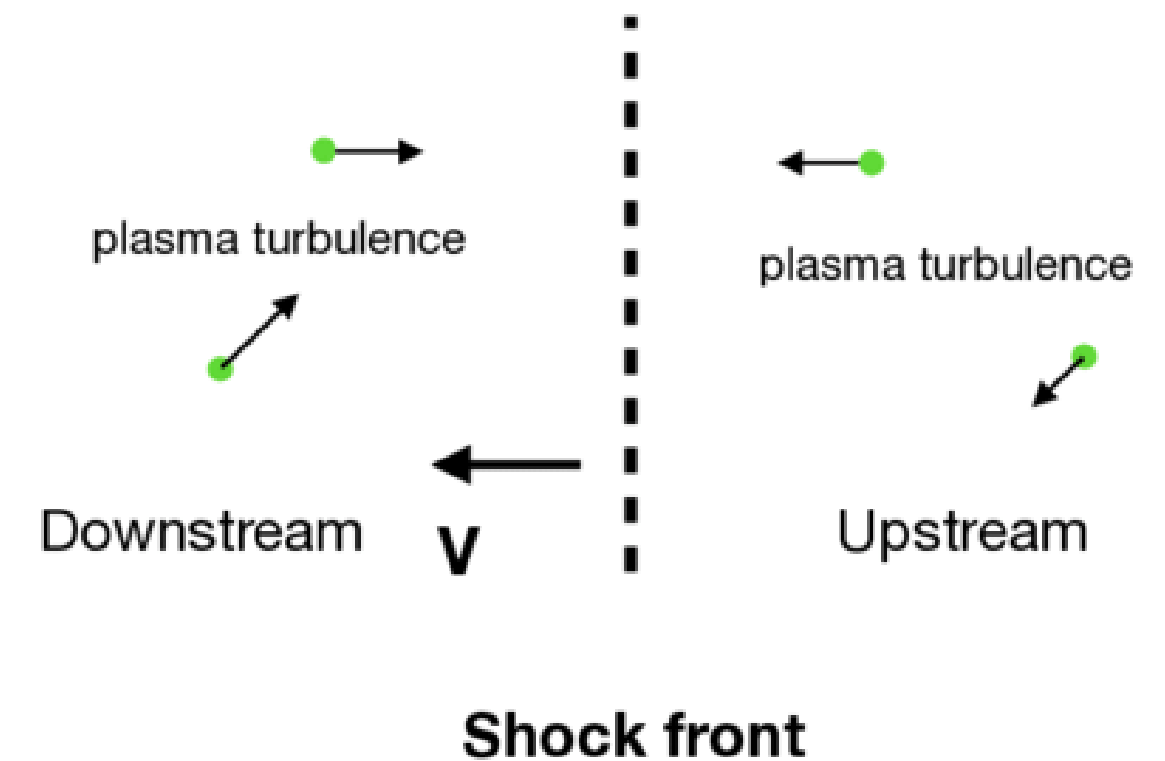


# PARTICLE ACCELERATION MECHANISMS WITHIN BLAZARS

## SHOCK ACCELERATION - FERMI I

Within the context of shock waves, there are several acceleration mechanisms namely:

- Shock drift acceleration (SDA)
- Shock surfing acceleration (SSA)
- Diffusive shock acceleration (DSA)

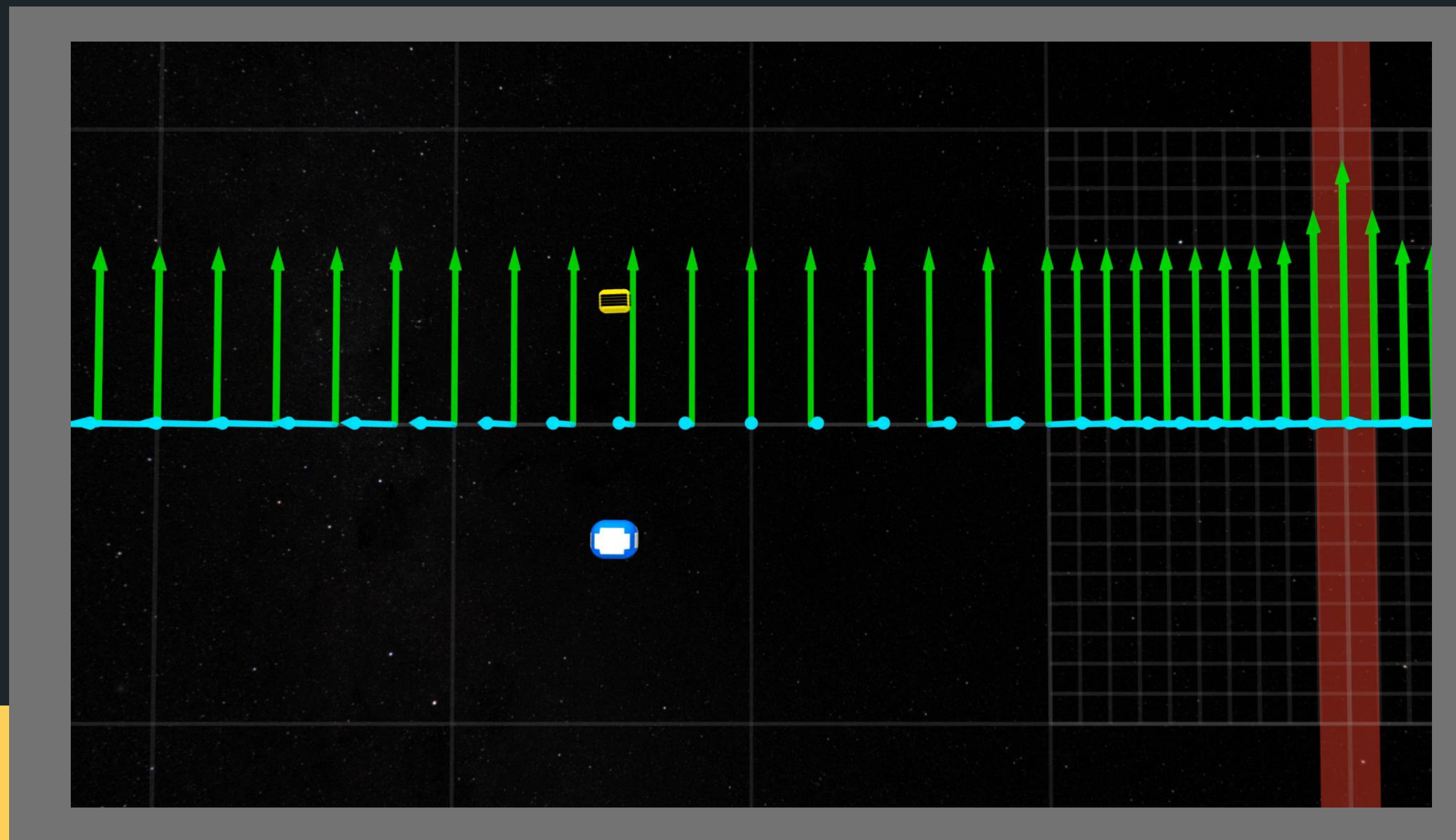


1st order Fermi-acceleration. Particles are accelerated by shock waves.

# SHOCK ACCELERATION - FERMI I

## SHOCK DRIFT ACCELERATION (DSA)

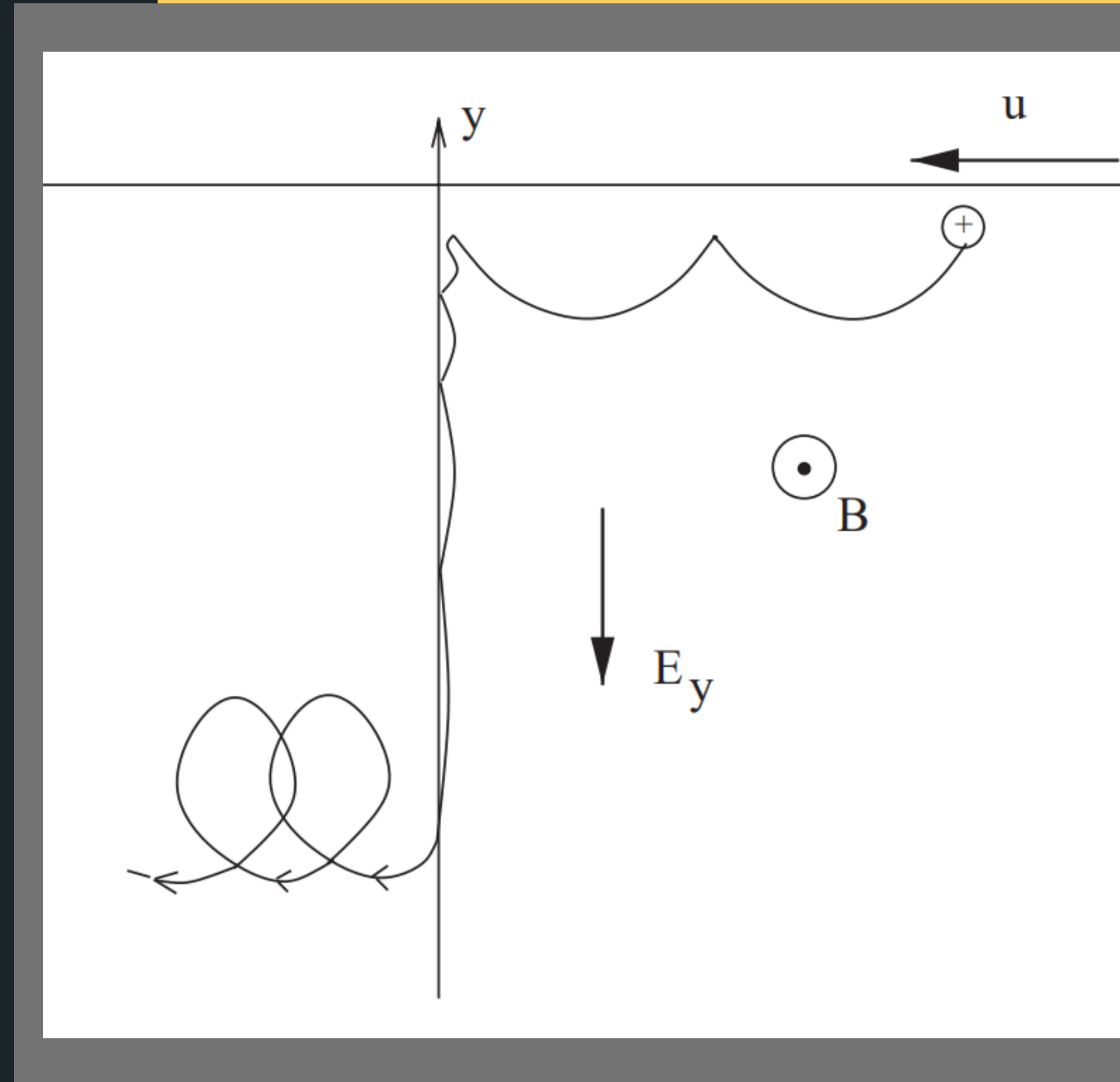
Shock drift acceleration occurs in quasi-perpendicular shocks and is based on the motion of particles along the shock front, and it can essentially be equated to a grad B drift resulting from the compression of the magnetic field across the shock front.



# SHOCK ACCELERATION - FERMI I

## SHOCK SURFING ACCELERATION (SSA)

Shock Surfing Acceleration is similar to SDA, with the distinction that it occurs when ions are reflected by the potential of the shock and then return to the shock front due to the upstream Lorentz force.

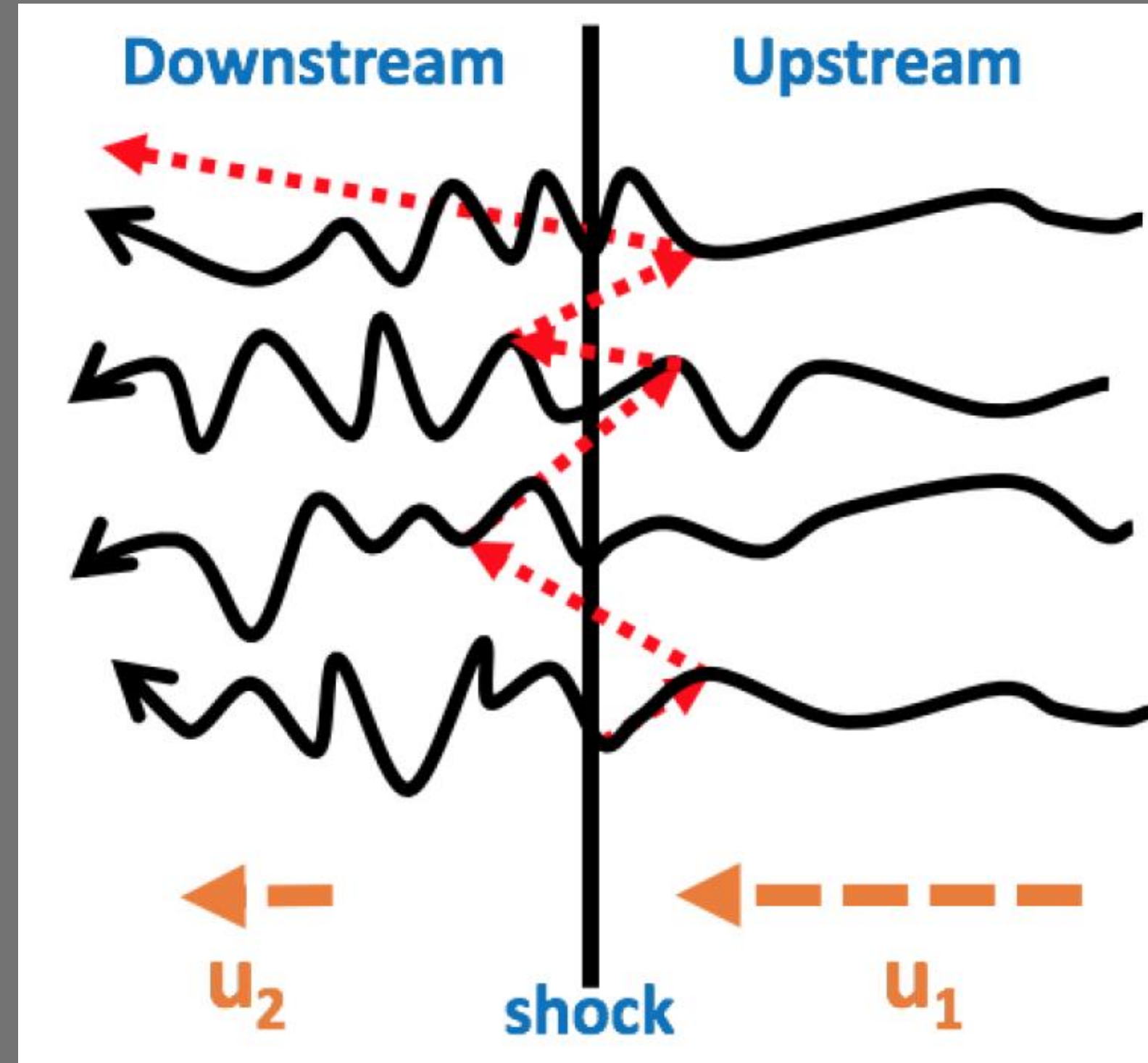


# SHOCK ACCELERATION - FERMI I

## DIFFUSIVE SHOCK ACCELERATION (DSA)

Particle energised via multiple scattering off magnetic disturbances present in both the upstream and downstream regions.

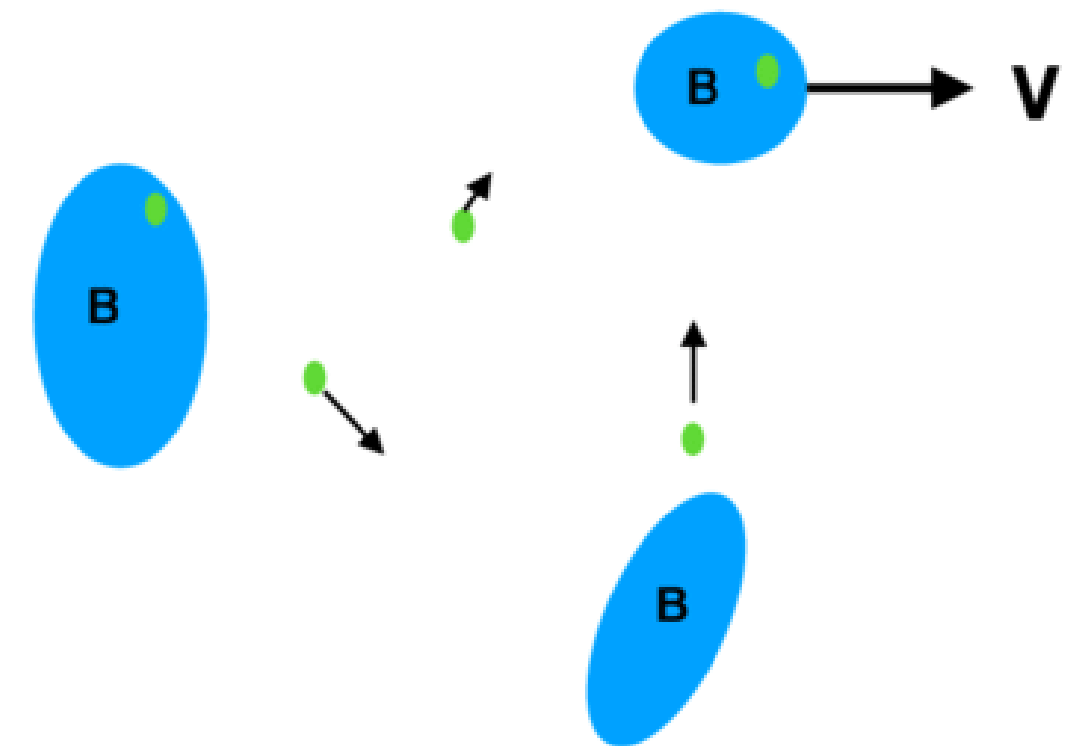
The presence of a shock allows for a situation in which collisions are always roughly head-on, although the actual scattering process is deflection off a turbulent magnetic field.



# PARTICLE ACCELERATION MECHANISMS WITHIN BLAZARS

## SECOND ORDER FERMI ACCELERATION - FERMI II

Mechanism through which particles can be accelerated due to stochastic collisions and/or scattering off magnetised clouds or turbulent velocity fields

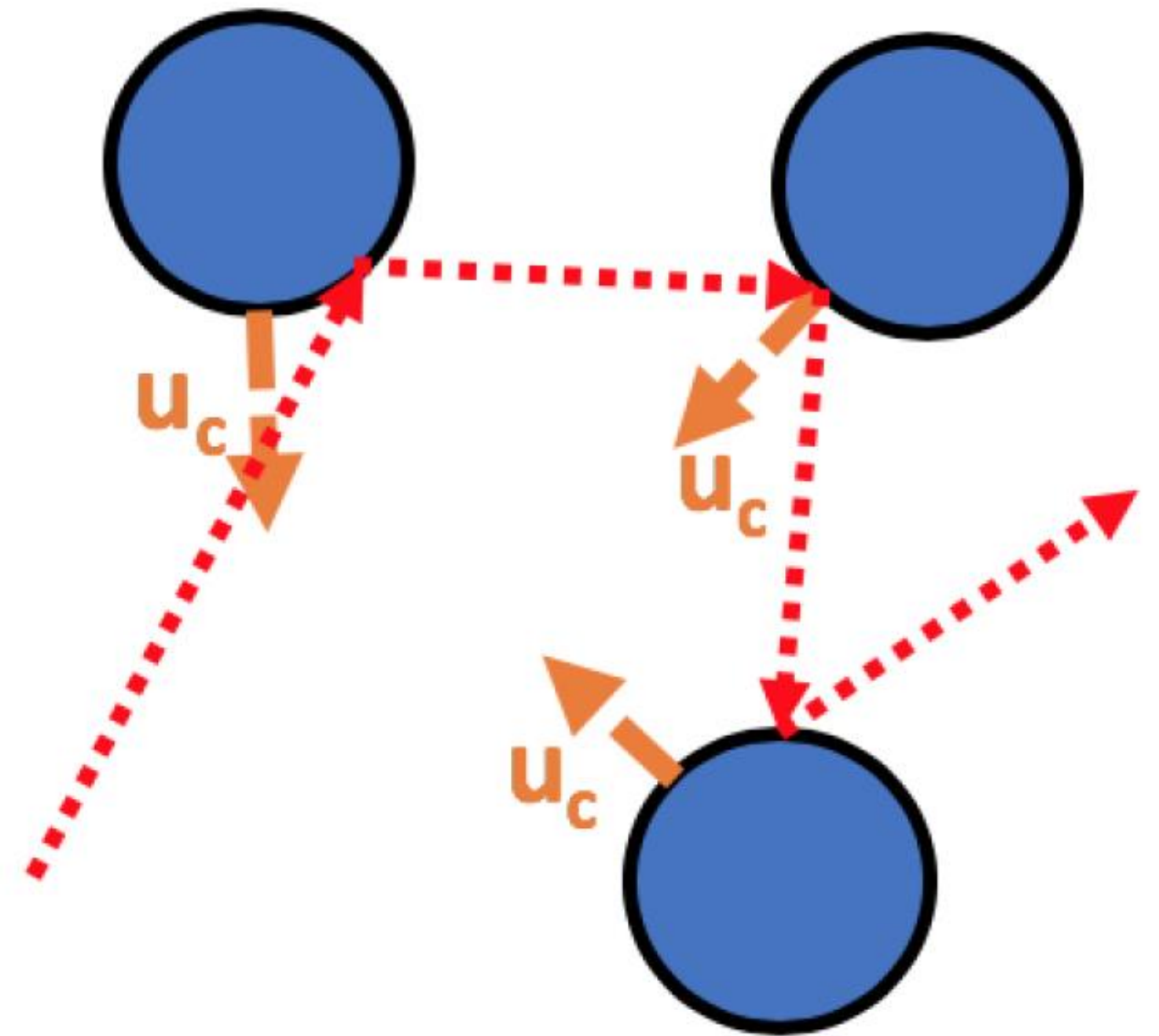


2nd order Fermi-acceleration.  
Cosmic rays are accelerated by  
random moving magnetic clouds.

# SECOND ORDER FERMI ACCELERATION - FERMI II

Fermi's initial approach took into consideration clouds moving at velocity  $u_c$ , serving as scatterers for particles which would either gain or lose a fraction  $\sim u_c/c$  of energy per collision.

The energy increase associated with this mechanism can be attributed to the prevalence of head-on collisions.

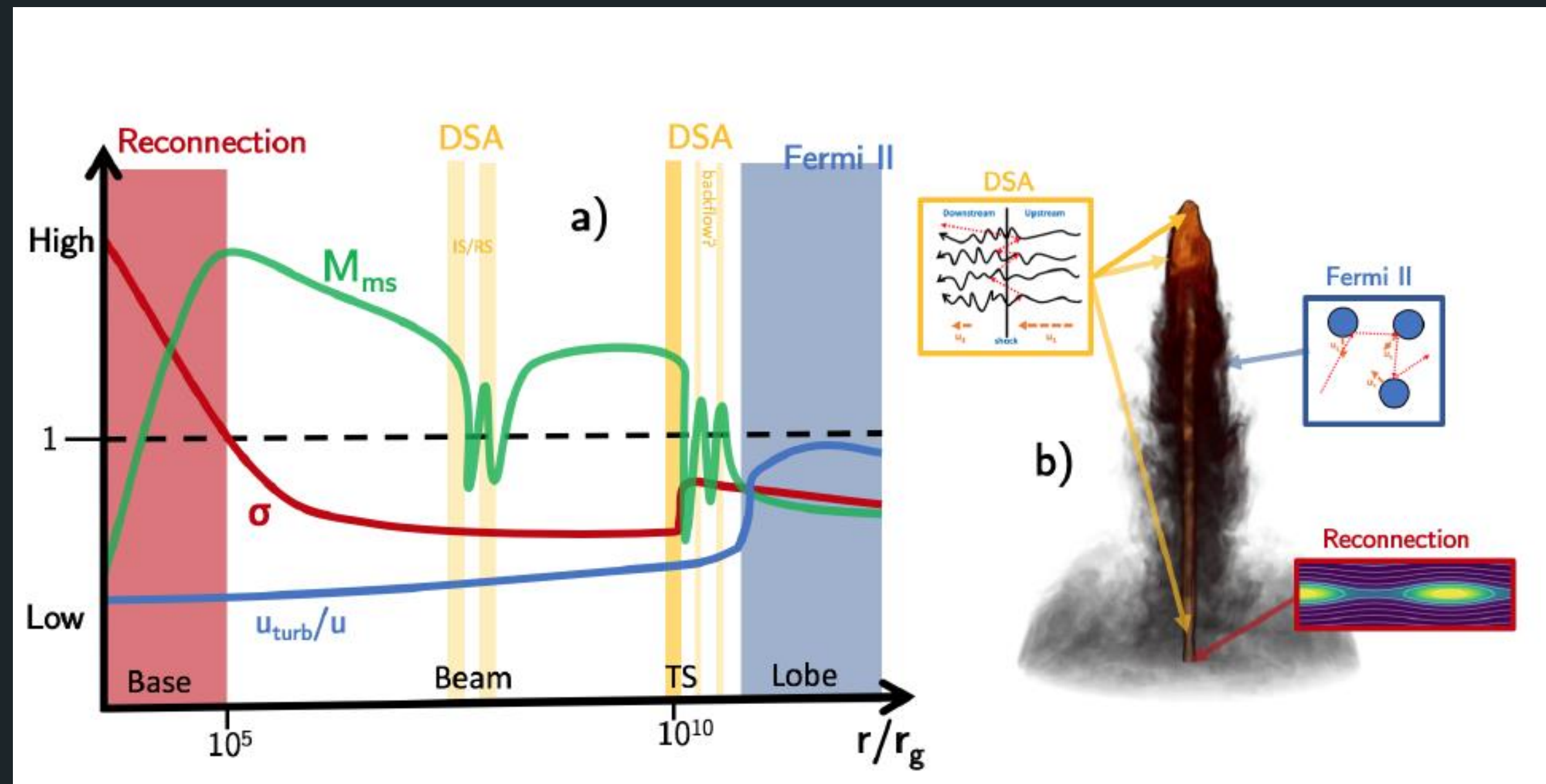


# PARTICLE ACCELERATION MECHANISMS WITHIN BLAZARS

## POSSIBLE PROFILE ALONG AN AGN JET

Mechanisms detailed thus far are those most invoked to explain the HE and VHE particles associated with blazars.

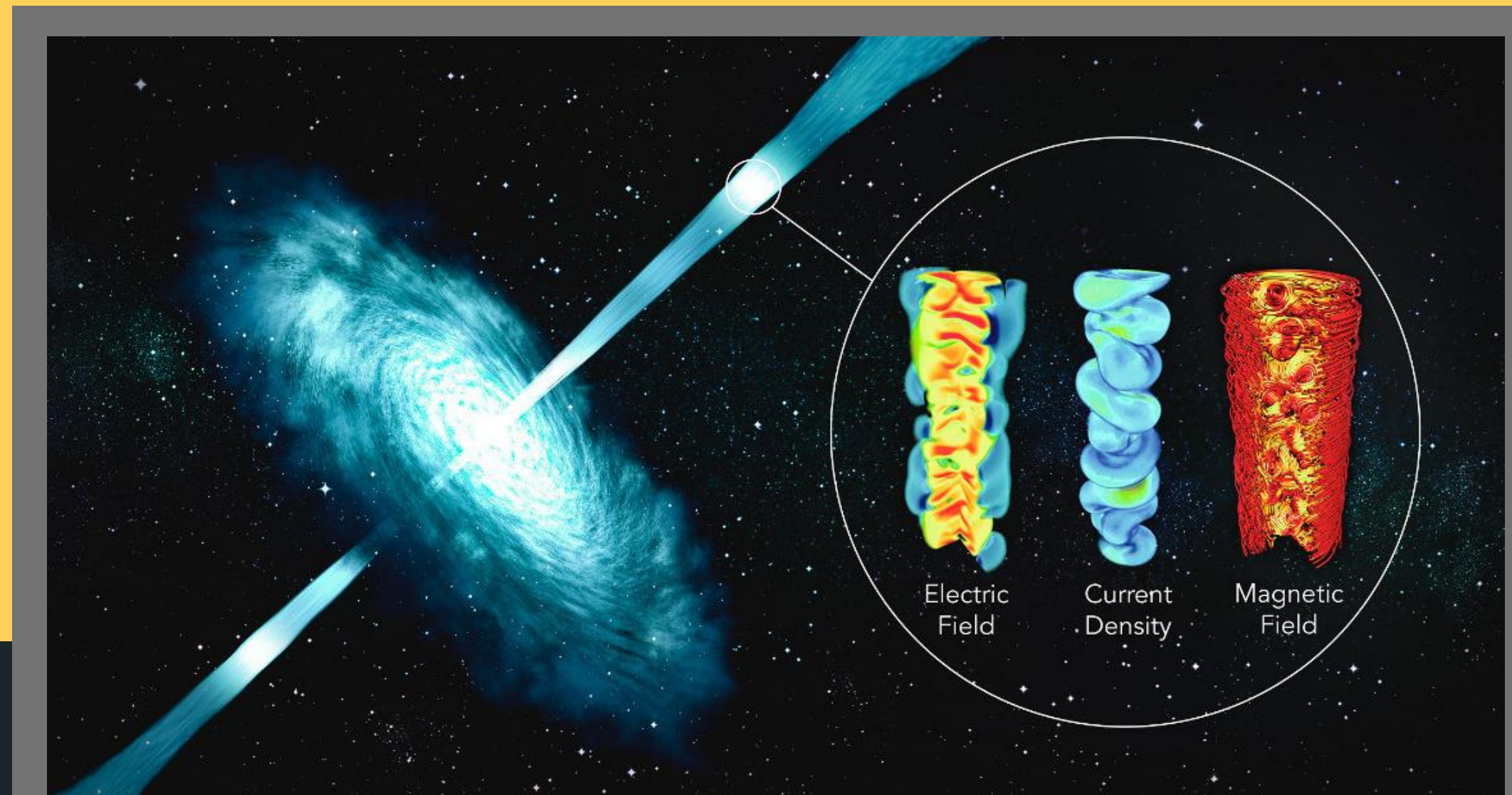
Example of a possible profile along an AGN jet, accompanied by a rendering of a jet tracer indicating the dominant mechanisms in each region.



# PARTICLE ACCELERATION MECHANISMS WITHIN BLAZARS

## OTHER MECHANISMS

Additional mechanisms exist which are also capable of accelerating particles to highly superthermal energies, i.e. shear acceleration, magnetic kink instabilities and extraction of rotational energy from rotational black holes.

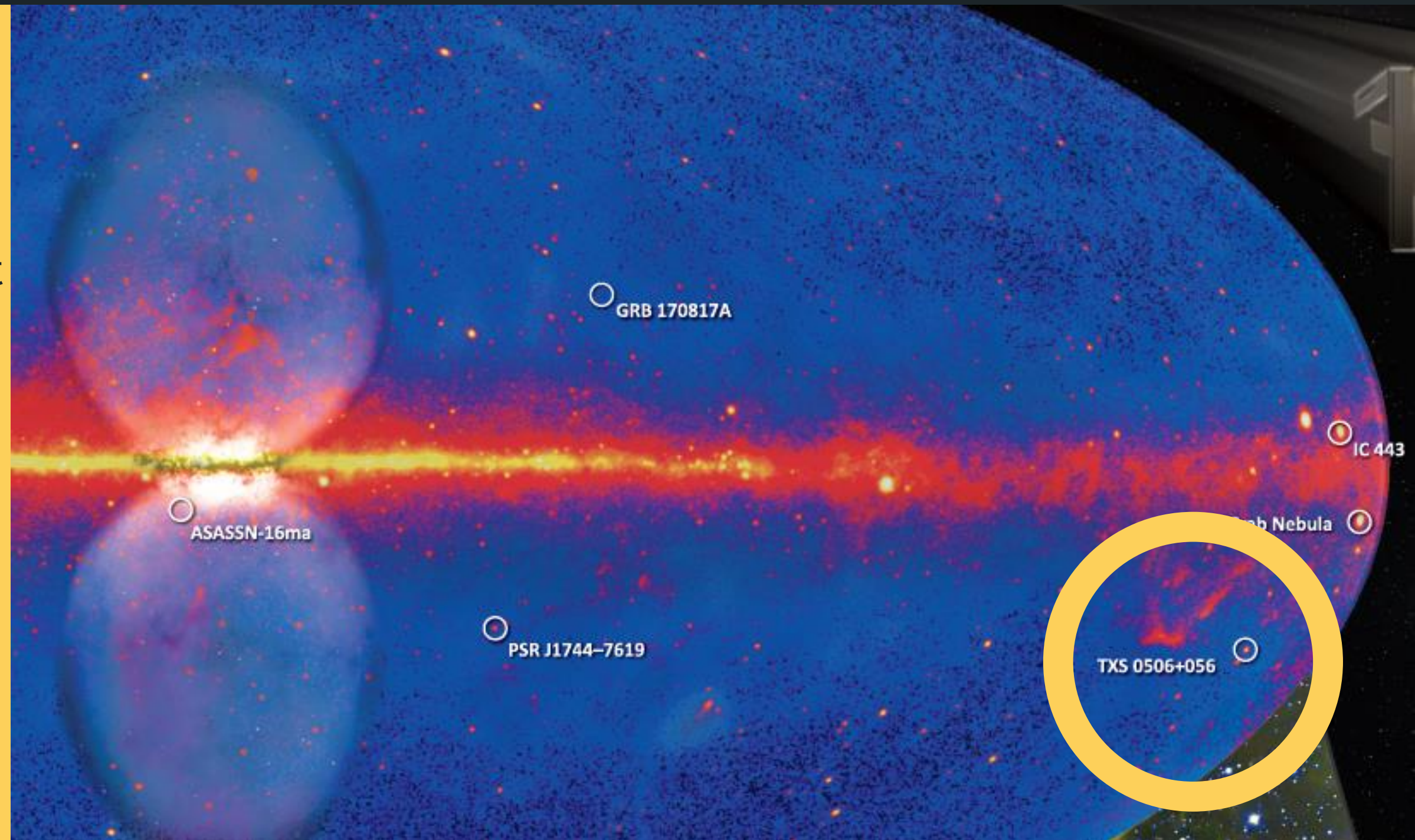


# PARTICLE ACCELERATION MECHANISMS WITHIN BLAZARS

## GAMMA-RAY EMISSION

Gamma-rays are electrically neutral, and as such their acceleration and emission cannot be attributed to the of the previously mentioned mechanisms.

Production of gamma-rays occurs via both leptonic and hadronic interactions



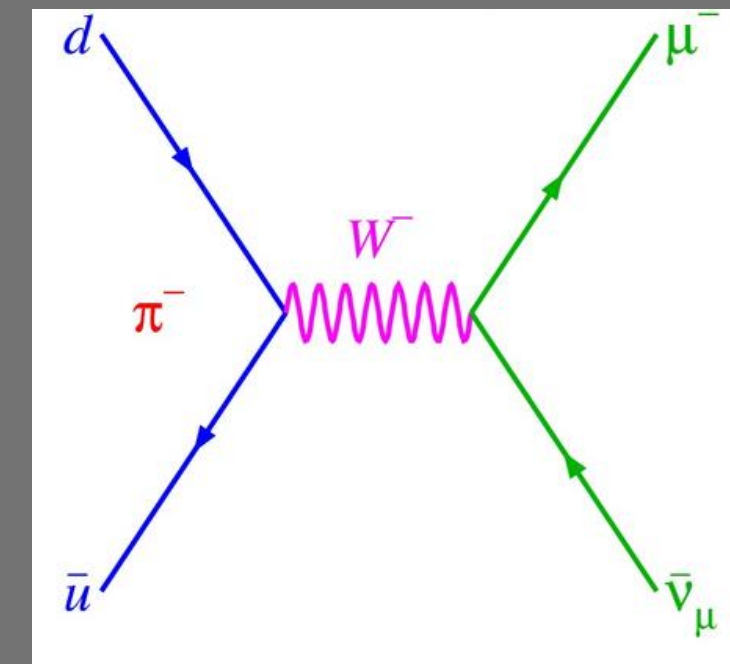
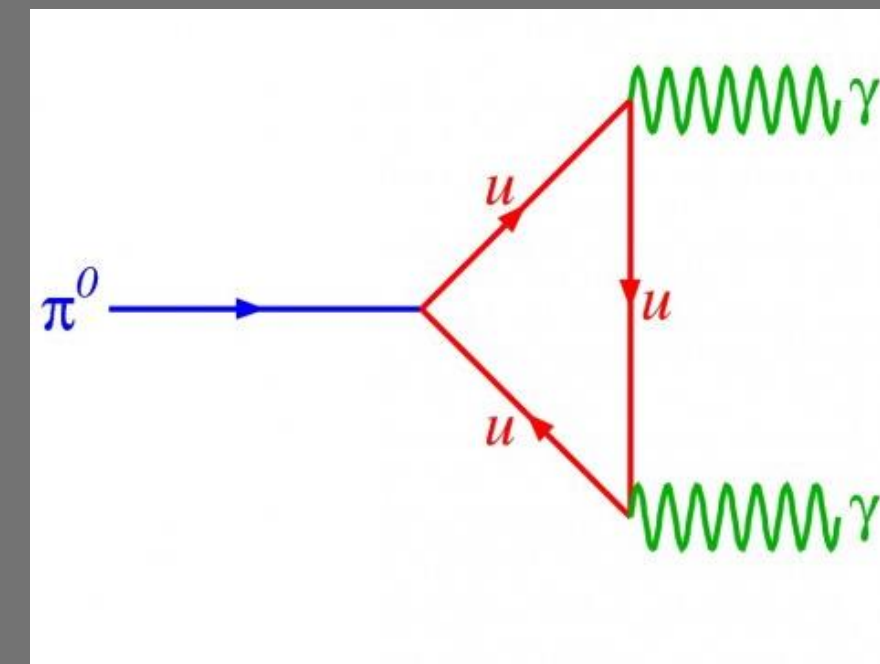
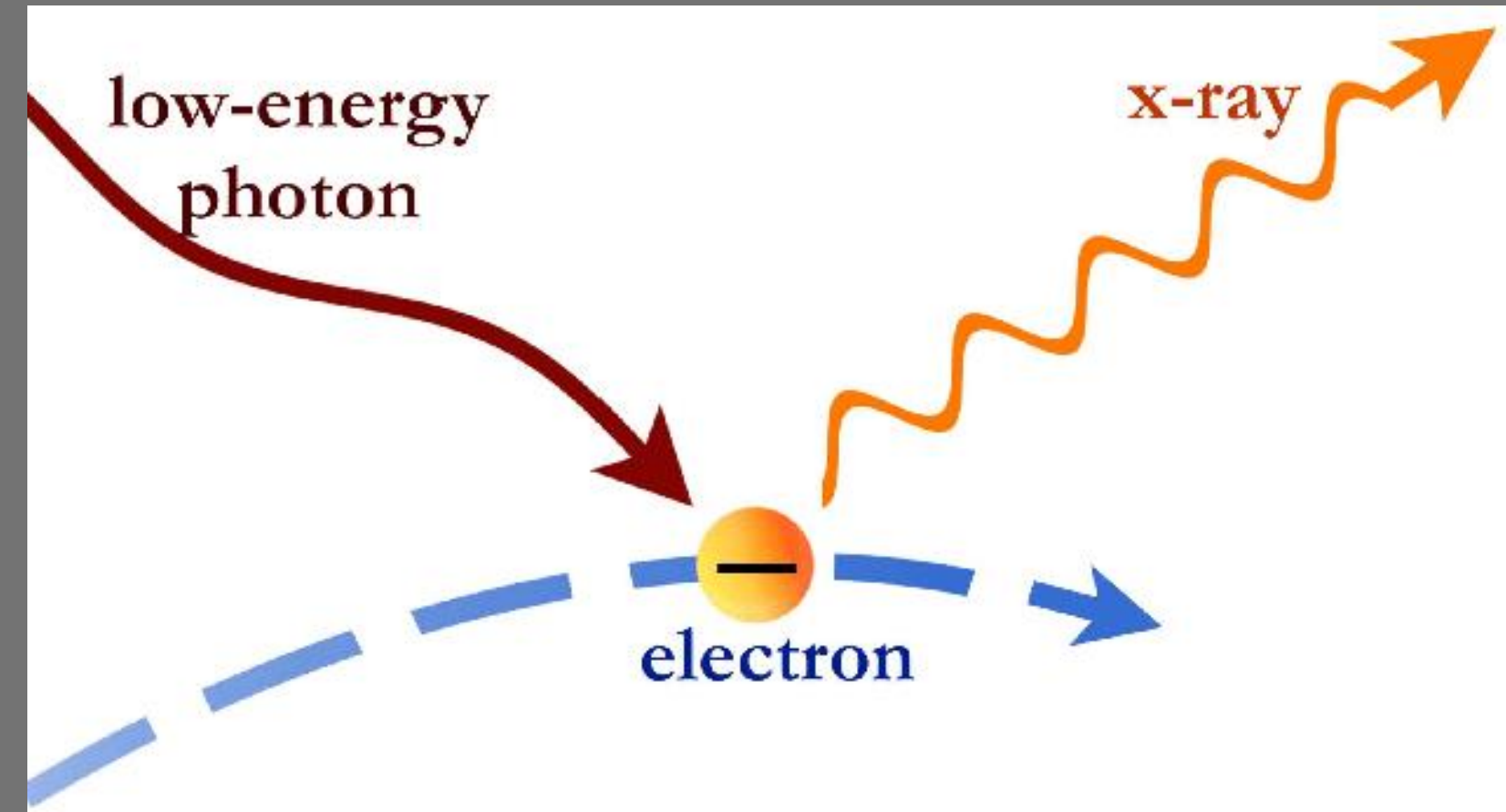
# GAMMA-RAY EMISSION

## LEPTONIC MECHANISMS

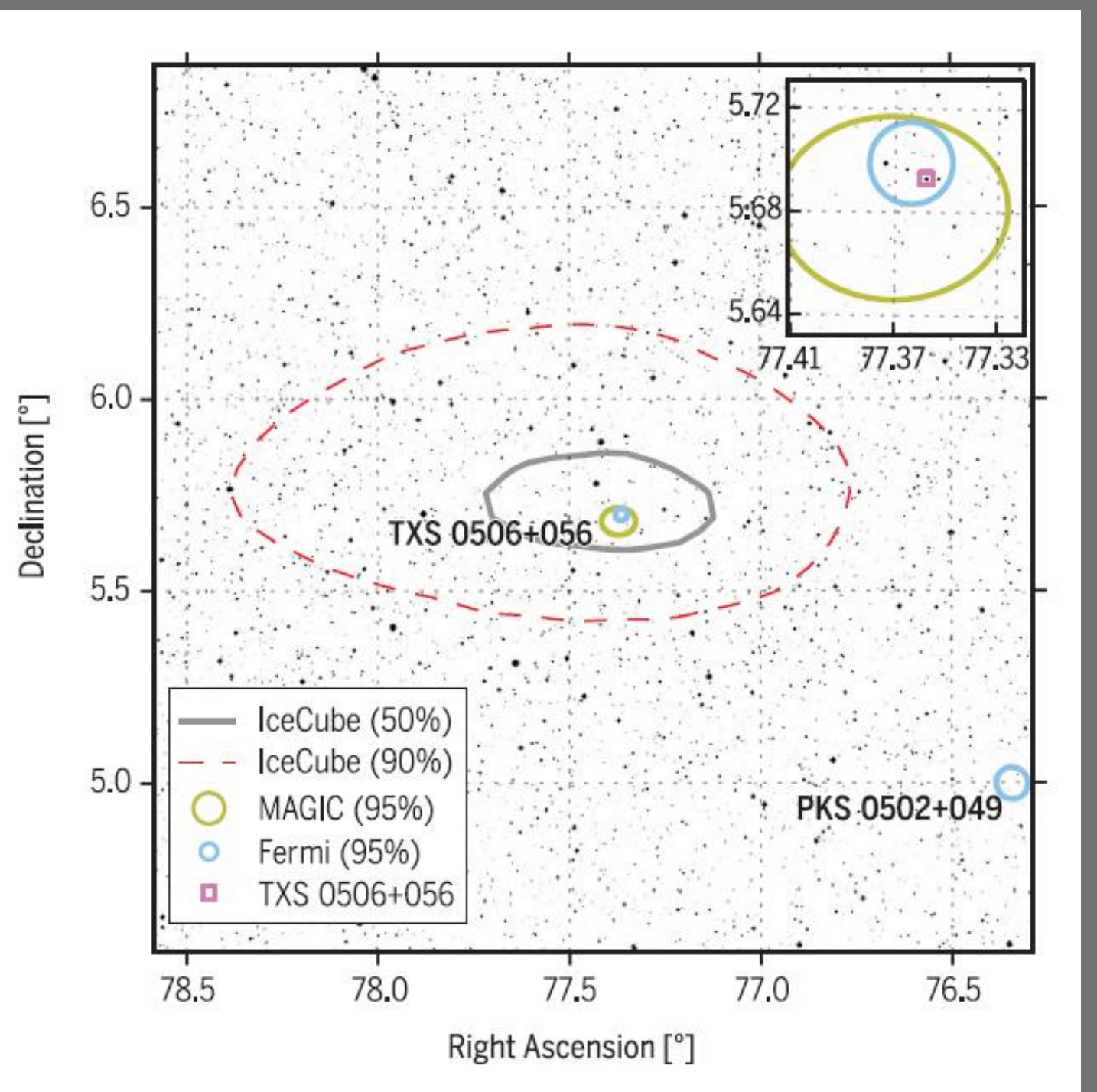
- Inverse Compton - high-energy particle interacts with a low-energy photon giving rise to a photon of higher energy.
- Includes interactions of energetic electrons with radiation fields or even with the electrons' own synchrotron radiation - **synchrotron self-Compton**.
- Synchrotron radiation

## HADRONIC MECHANISMS

Production via interactions between high-energy protons with other protons, photons or magnetic fields. Generates pions, which can decay into photons and/or neutrinos



# EXPERIMENTAL EFFORTS



## TXS 0506+056 BLAZAR AND THE ICECUBE-170922A NEUTRINO EVENT

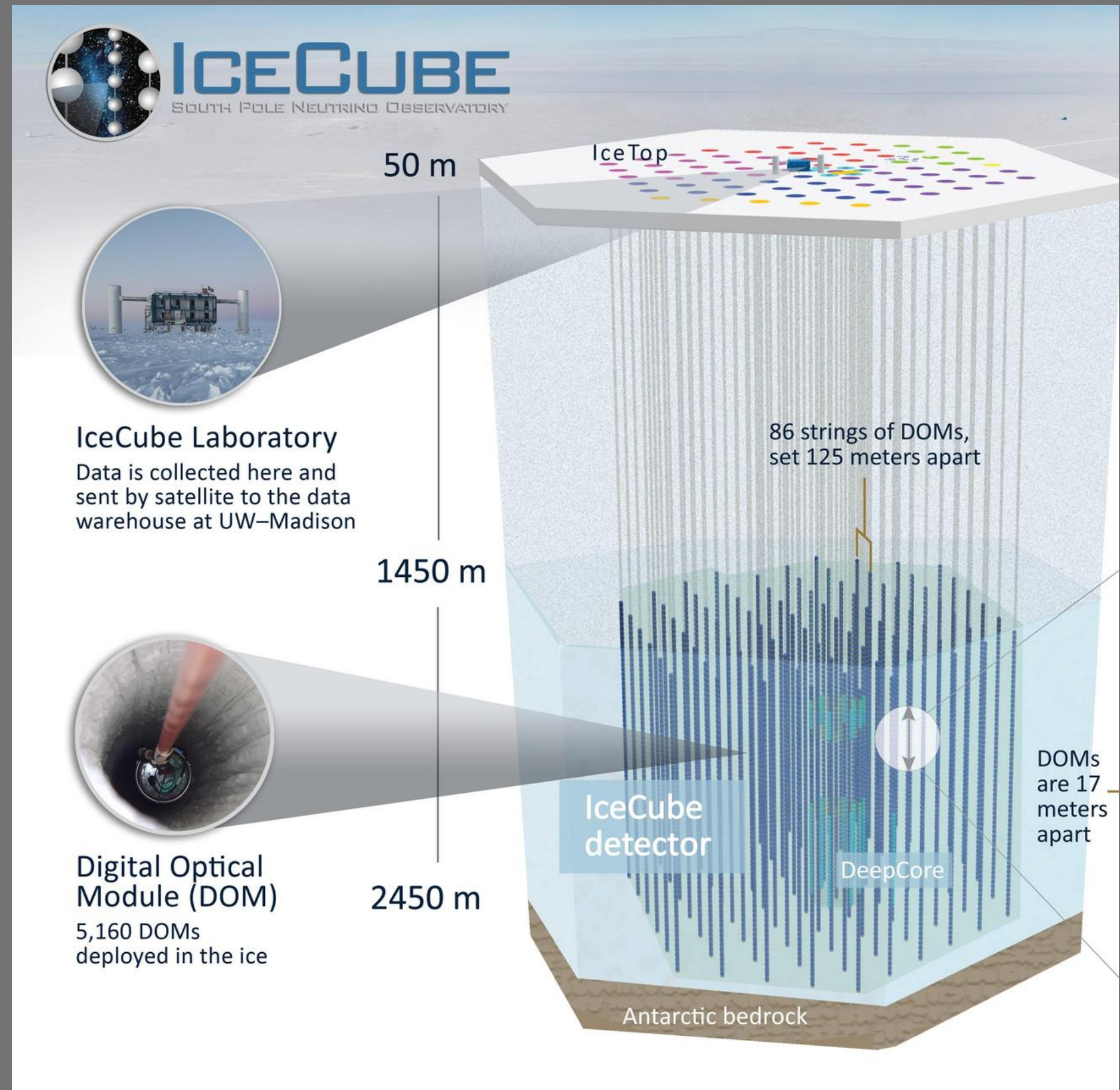
Multimessenger and multiwavelength observation of the TXS 0506+056 flaring blazar, in spatial coincidence with the high-energy neutrino IceCube-170922A.

# ICECUBE NEUTRINO OBSERVATORY

Cubic-kilometre-sized neutrino detector, placed deep in the ice of the geographic South Pole.  
Between depths of 1450m and 2450m .

Particle detection performed by a set of 5160 digital optical modules (DOMs).

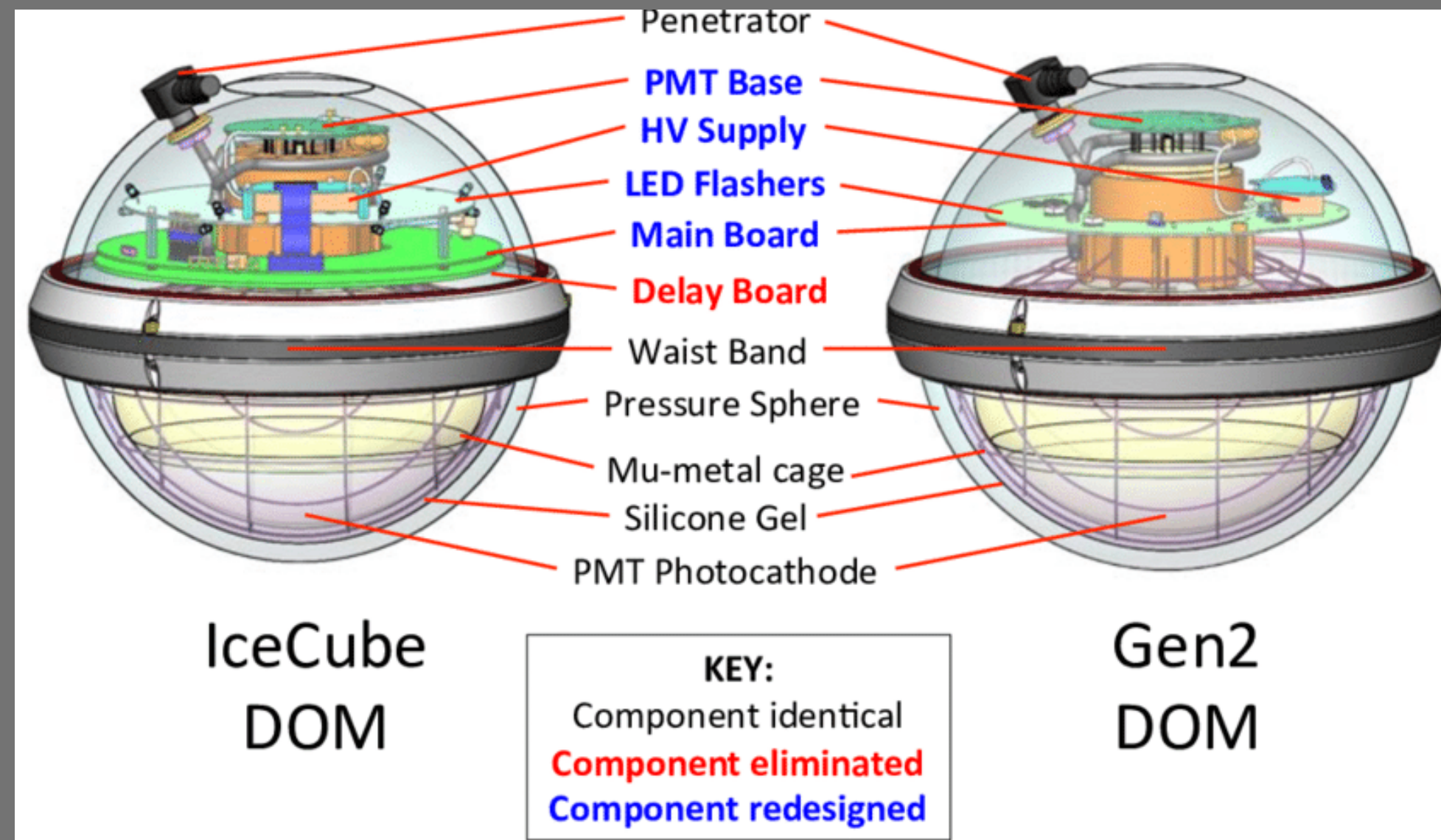
Does not directly observe neutrinos, it detects the secondary particles produced by the interaction of neutrinos with matter.



# ICECUBE NEUTRINO OBSERVATORY

## TRIGGER FOR NEUTRINO ALERT

- Primary trigger defined as 8 DOMs registering photon signals within a  $5\mu\text{s}$  window.
- If criterion is met: DAQ records all signals within a  $+6/-4\mu\text{s}$  window around the trigger time, grouping all information into a single event.



# ICECUBE-170922A

## SYSTEMATIC UNCERTAINTIES

Directional resolution of muon tracks limited mainly by:

- Stochastic nature of detected Cherenkov light;
- Finite density of DOMs which detect light;
- Uncertainty in the optical properties of the glacial ice.

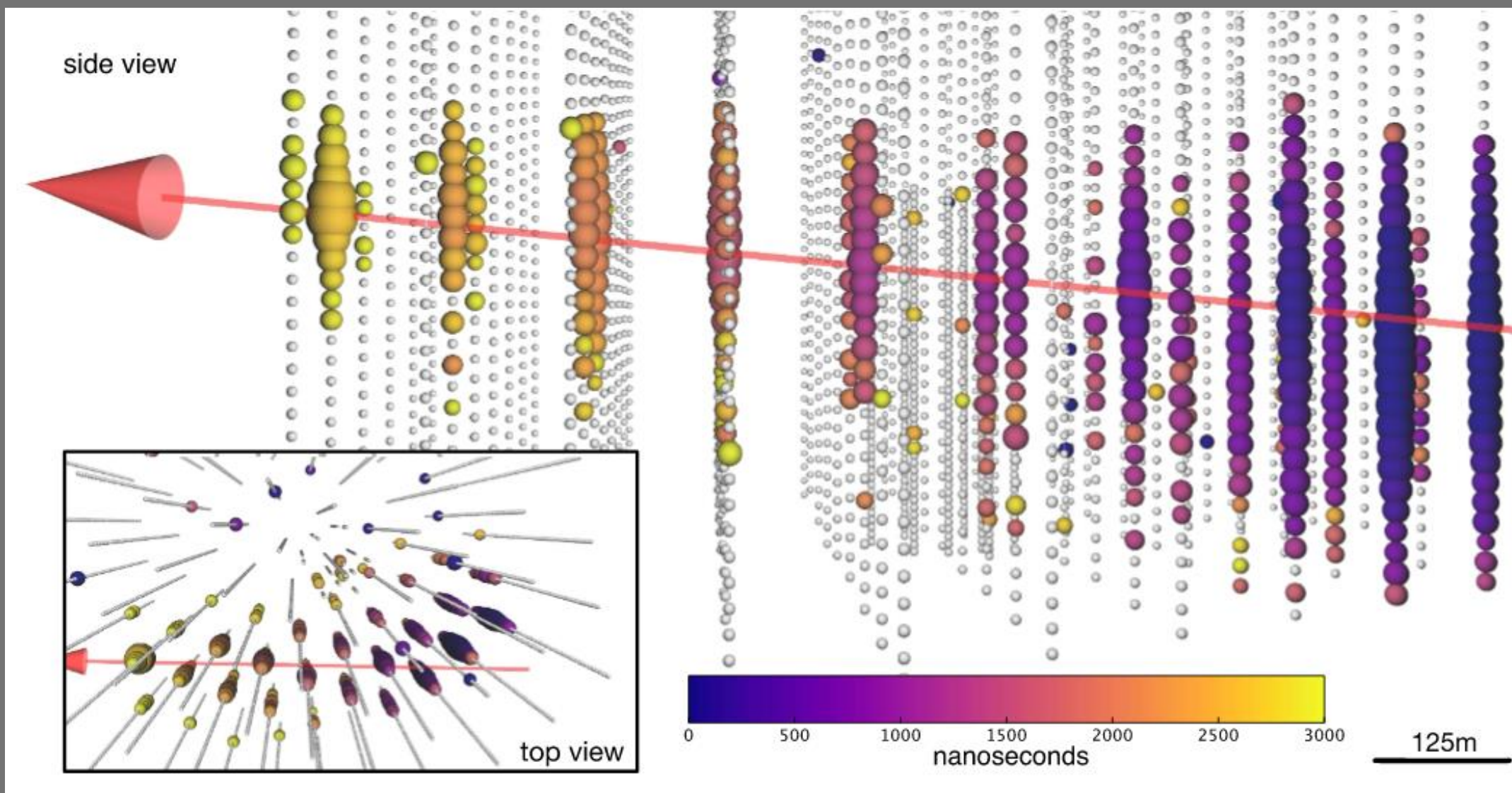
Expected uncertainty due to statistical and systematic effects modeled via simulations of large samples of candidate events resembling the observed event.

# ICECUBE ALERT SYSTEM

## EVENT PROCESSING AND RECONSTRUCTION

Online processing and filtering system distributes the gathered events amongst the members of a farm of around 400 calibration and filtering client processors.

System also makes use of reconstruction algorithms to characterise the information extracted from the conditions of Cherenkov light generation associated with each event.

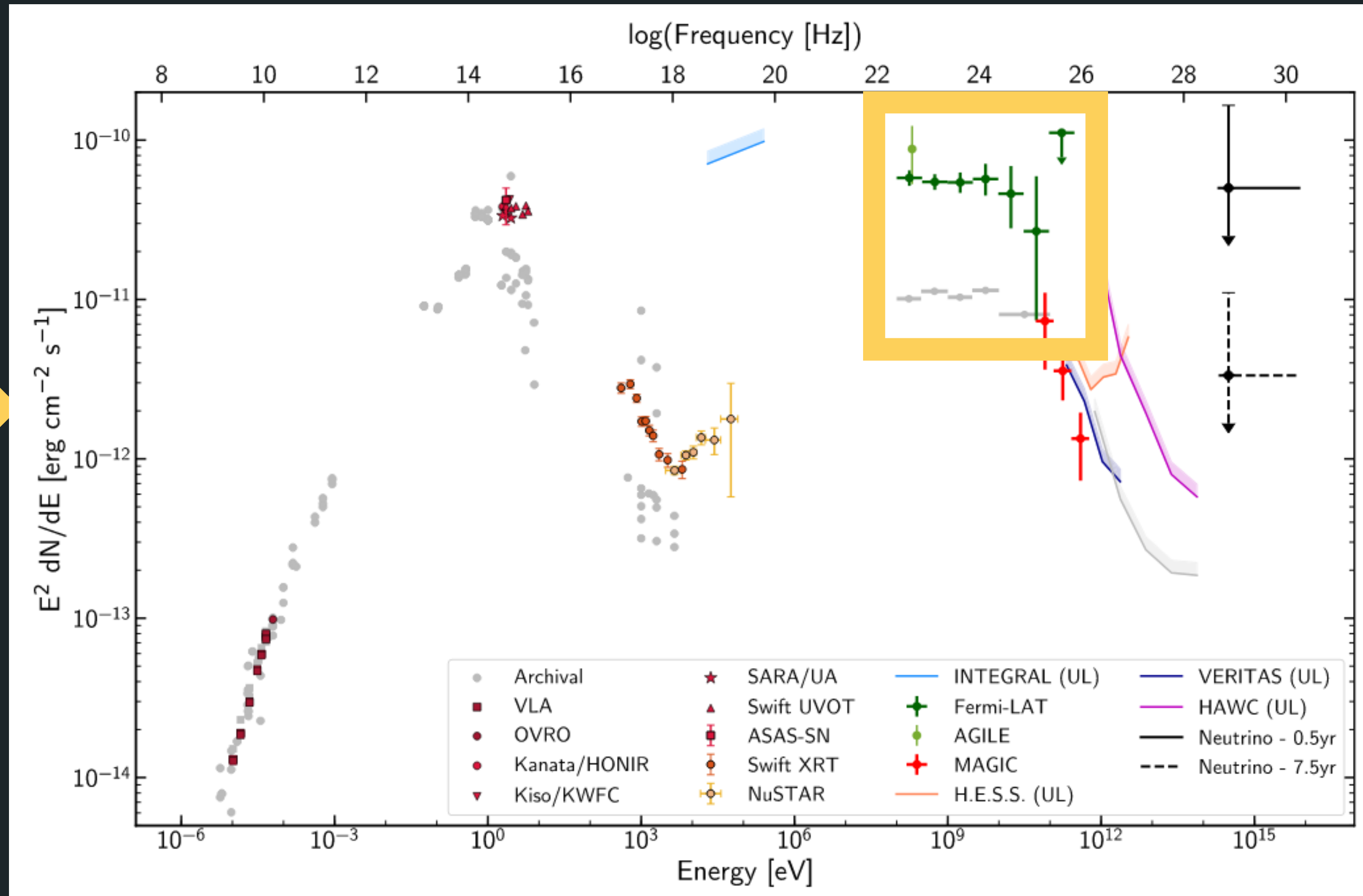


# SED OF TXS 0506+056

## THE GAMMA RAYS

Fermi -LAT reported that the origin region of the IceCube-170922A neutrino was consistent with the position of the TXS0506+056 blazar, included in three catalogues of Fermi sources at energies above 0.1, 50 and 10 GeV.

Fermi-LAT measured an average  $\gamma$ -ray flux of TXS 0506+056 for  $E > 0.1$  GeV of  $(7.6 \pm 0.2) \times 10^{-8} \text{ cm}^{-2} \text{ s}^{-1}$ .



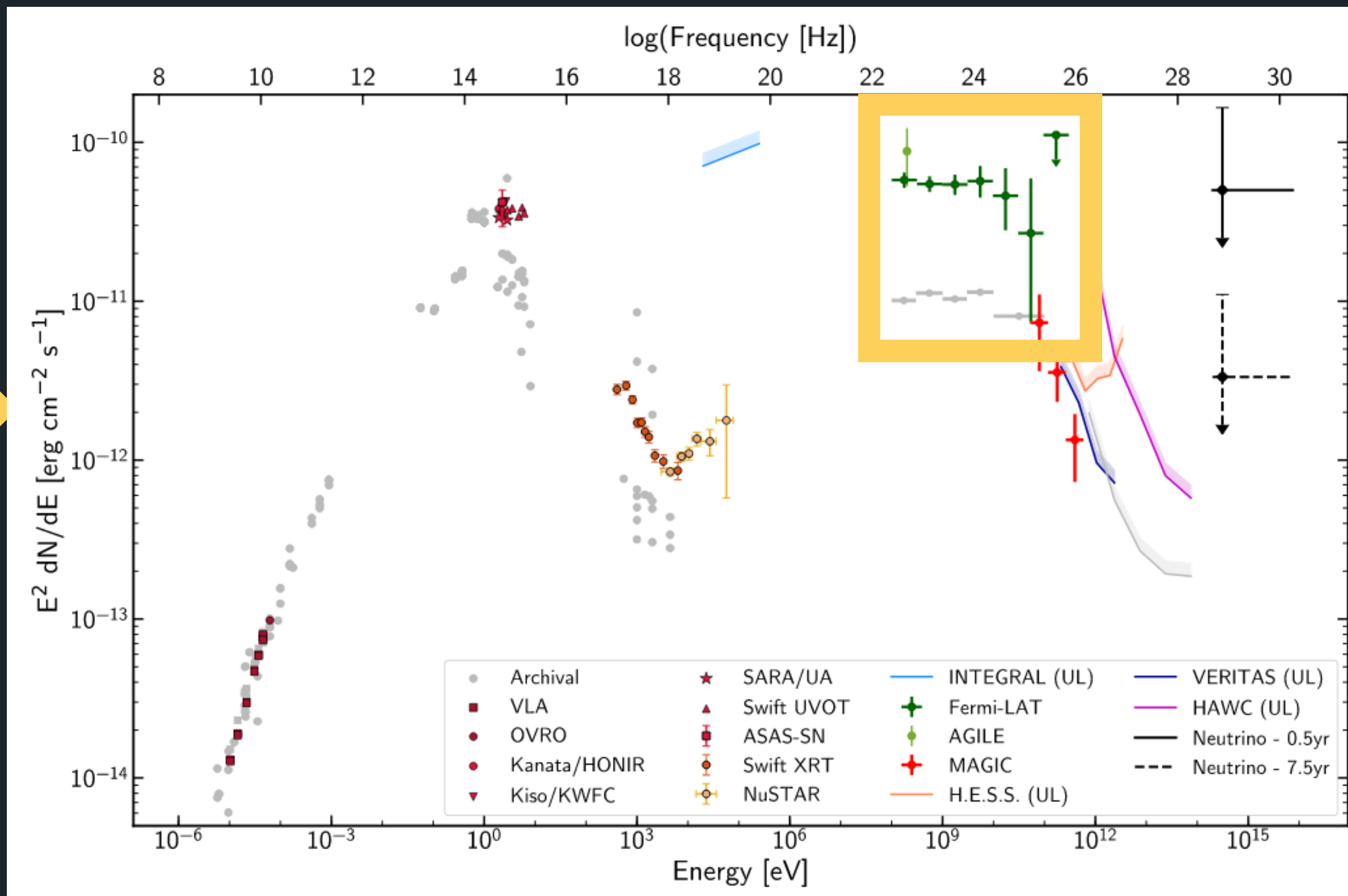
# SED OF TXS 0506+056

## HE GAMMA RAYS

AGILE: measured a flux of  $(5.3 \pm 2.1) \times 10^{-7} \text{ cm}^{-2} \text{ s}^{-1}$

during the 13-day window spanning from 10 to 23

September 2017, in agreement with Fermi-LAT observations

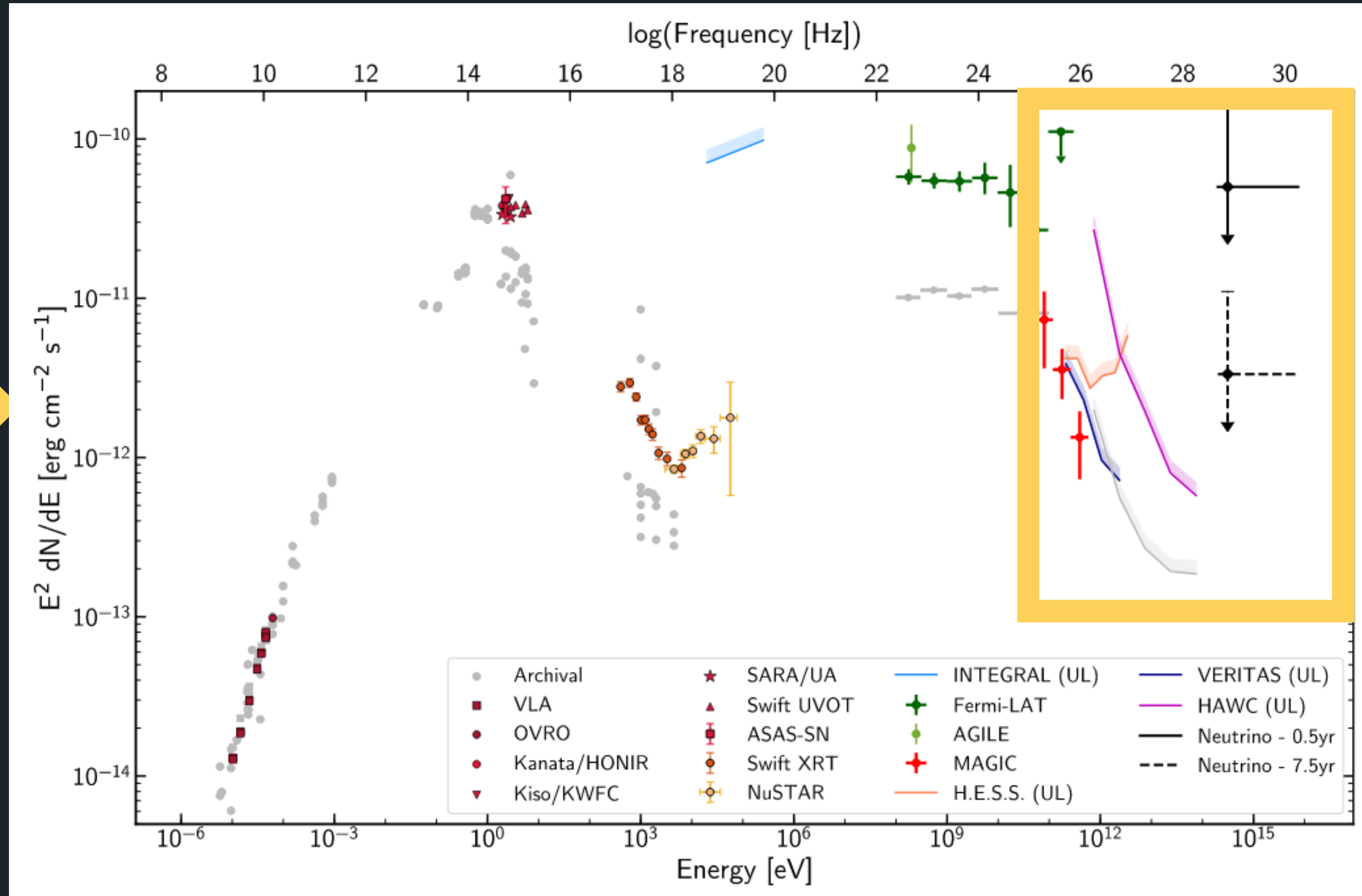


# SED OF TXS 0506+056

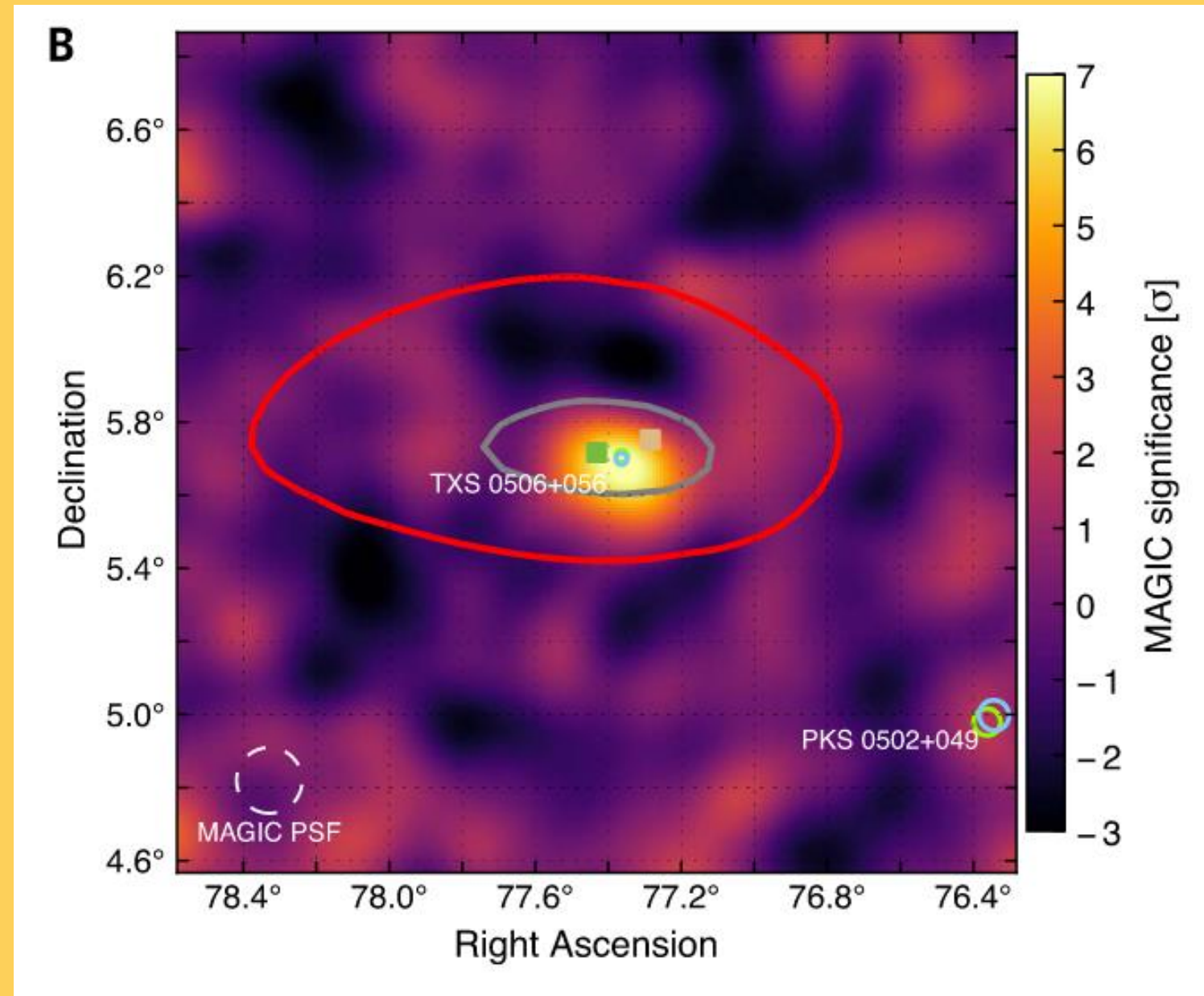
## VHE GAMMA RAYS

MAGIC : during the initial observations, no  $\gamma$ -ray emission was detected, and an upper limit of  $3.56 \times 10^{-7} \text{ cm}^{-2} \text{ s}^{-1}$  at 95% CL for the flux over 90 GeV.

Later observations resulted in the detection of hints of a VHE  $\gamma$ -ray signal, with an excess observed at  $3.5\sigma$  significance.

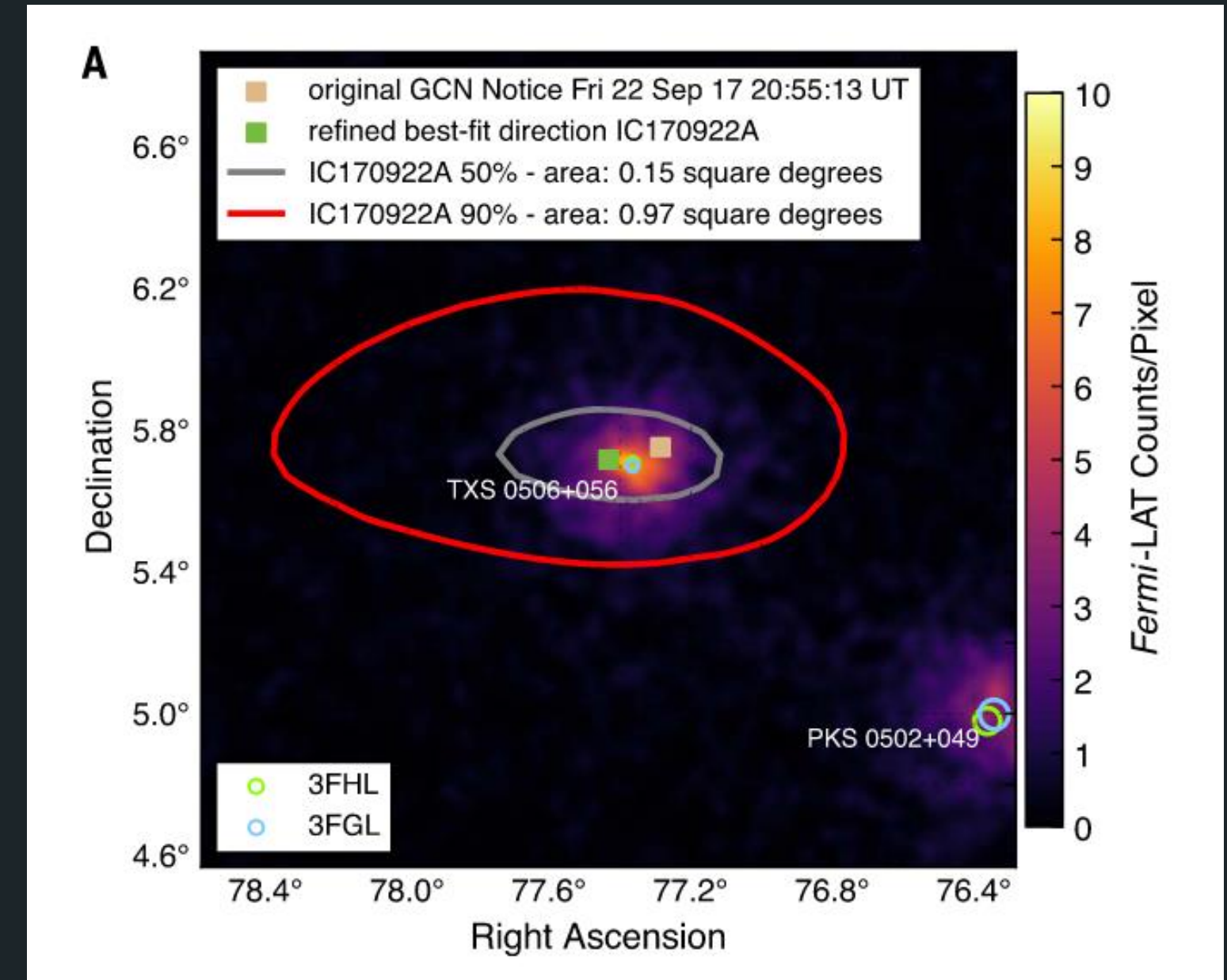


# OBSERVATIONS OF TXS 0506+056



## MAGIC

Signal significance as observed by MAGIC, for  $\gamma$ -rays above 90 GeV.



## FERMI-LAT

Location of IceCube-170922A in J2000 equatorial coordinates, overlaid with the  $\gamma$ -ray counts from Fermi-LAT above 1 GeV. 28

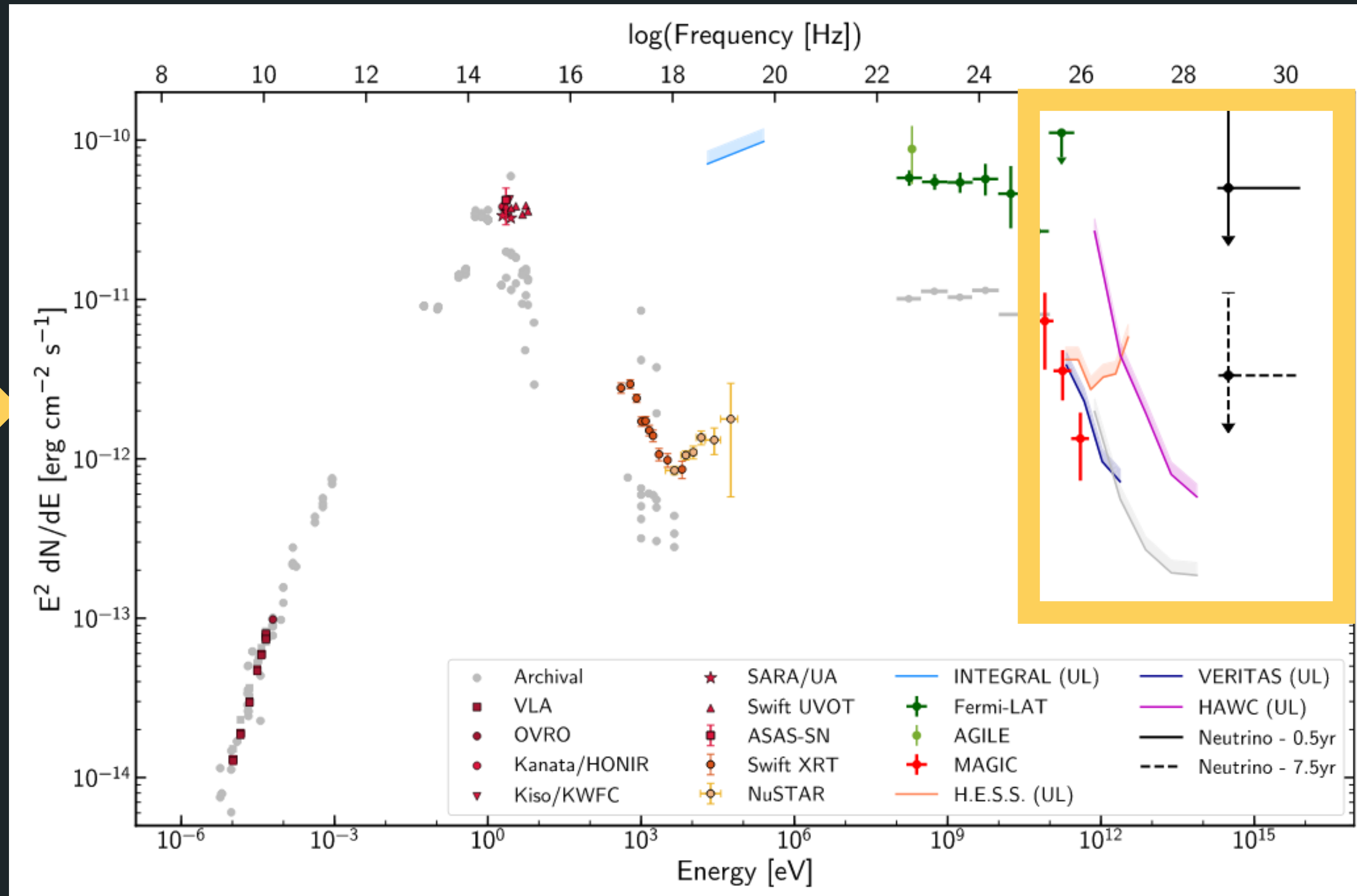
# SED OF TXS 0506+056

## VHE GAMMA RAYS

**HESS:** preliminary analysis did not reveal significant  $\gamma$ -ray emission

Observations following Fermi-LAT announcement also detected no significant  $\gamma$ -ray emission.

Upper limit at 95%CL on the  $\gamma$ -ray flux, yielded a value of  $7.5 \times 10^{-12} \text{ cm}^{-2} \text{ s}^{-1}$  for energies  $E > 175 \text{ GeV}$ .

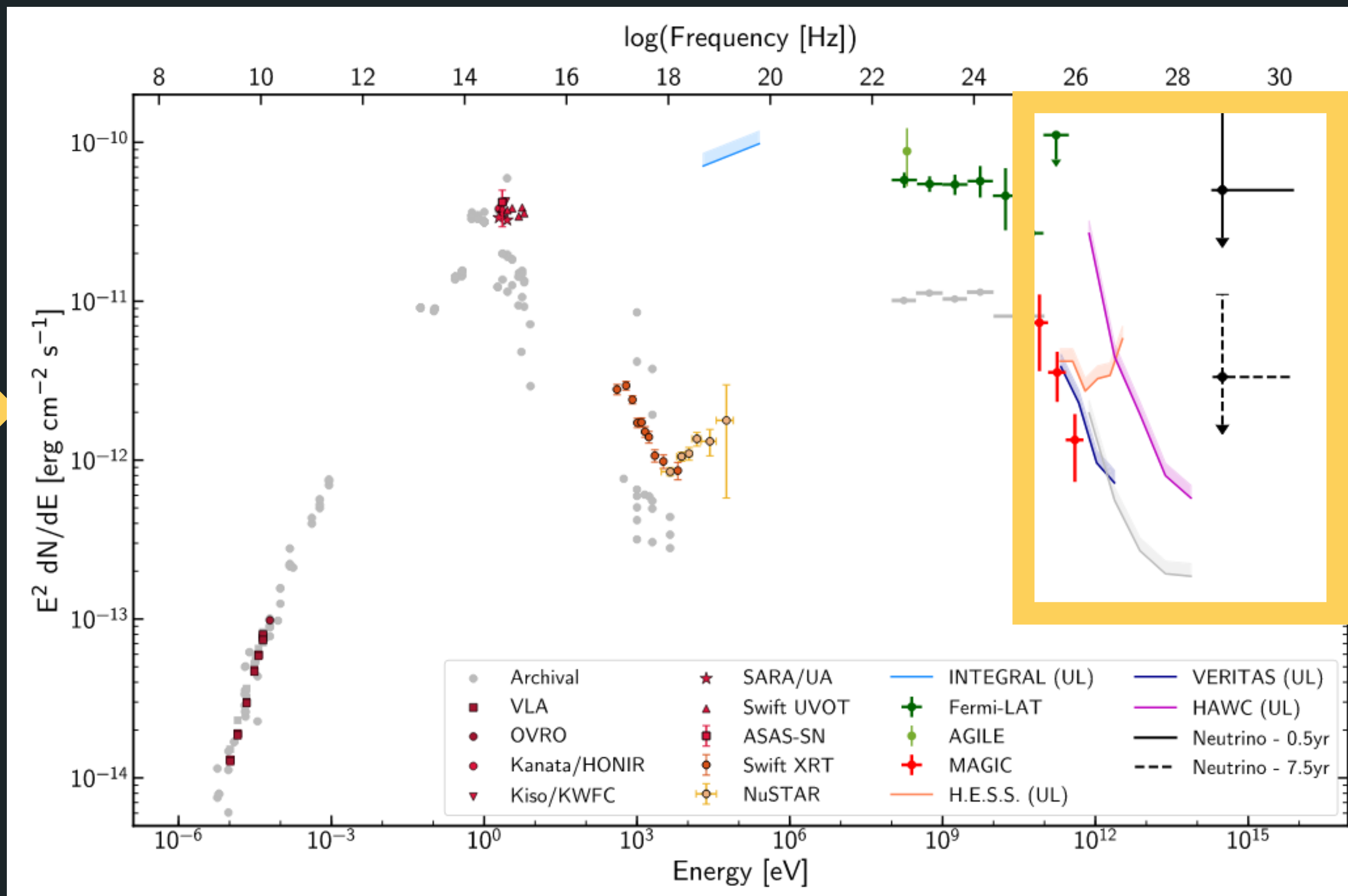


# SED OF TXS 0506+056

## VHE GAMMA RAYS

VERITAS : analysis of the data gathered showed no evidence of  $\gamma$ -ray emission at the location of the TXS 0506+056 blazar.

An upper limit on the integral  $\gamma$ -ray flux of  $1.2 \times 10^{-11} \text{ cm}^{-2} \text{ s}^{-1}$  at 95% CL was derived, for energies  $E > 175 \text{ GeV}$ .



# SED OF TXS 0506+056

## RADIO OBSERVATIONS

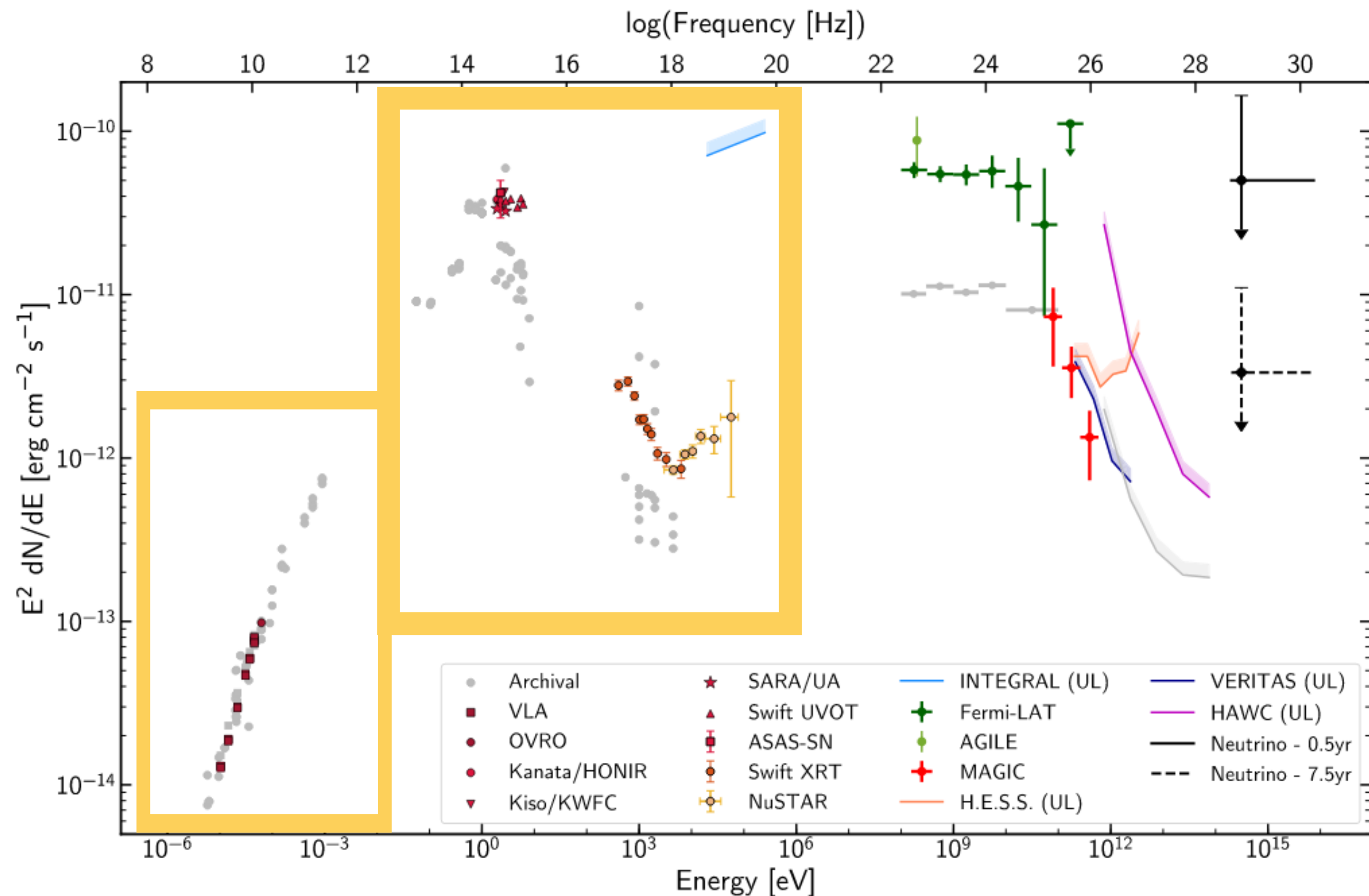
Contributions mainly from VLA, in the range 2-12 GHz, and OVRO.

## OPTICAL OBSERVATIONS

Contributions from ASAS-SN, Liverpool telescope, HONIR, KWFC, SALT, FOCAS

## X-RAY OBSERVATIONS

Contributions from XRT, GSC, NuSTAR and INTEGRAL



# NEUTRINO-BLAZAR COINCIDENCE ANALYSIS

- Aims to calculate, or constrain the chance probability of coincidence between the neutrino alert and the blazar.
- **Coincidence probability:** measure of the likelihood that the neutrino-blazar association can be attributed to chance.
- Test statistic (TS) is created to be used in a likelihood ratio test, to compare the signal hypothesis with the null hypothesis.
- **Null hypothesis:** no correlation between the known  $\gamma$ -ray sources and neutrino alerts,
- **Signal hypothesis:** neutrino events originate from blazars recorded in Fermi-LAT catalogues

# NEUTRINO-BLAZAR COINCIDENCE ANALYSIS

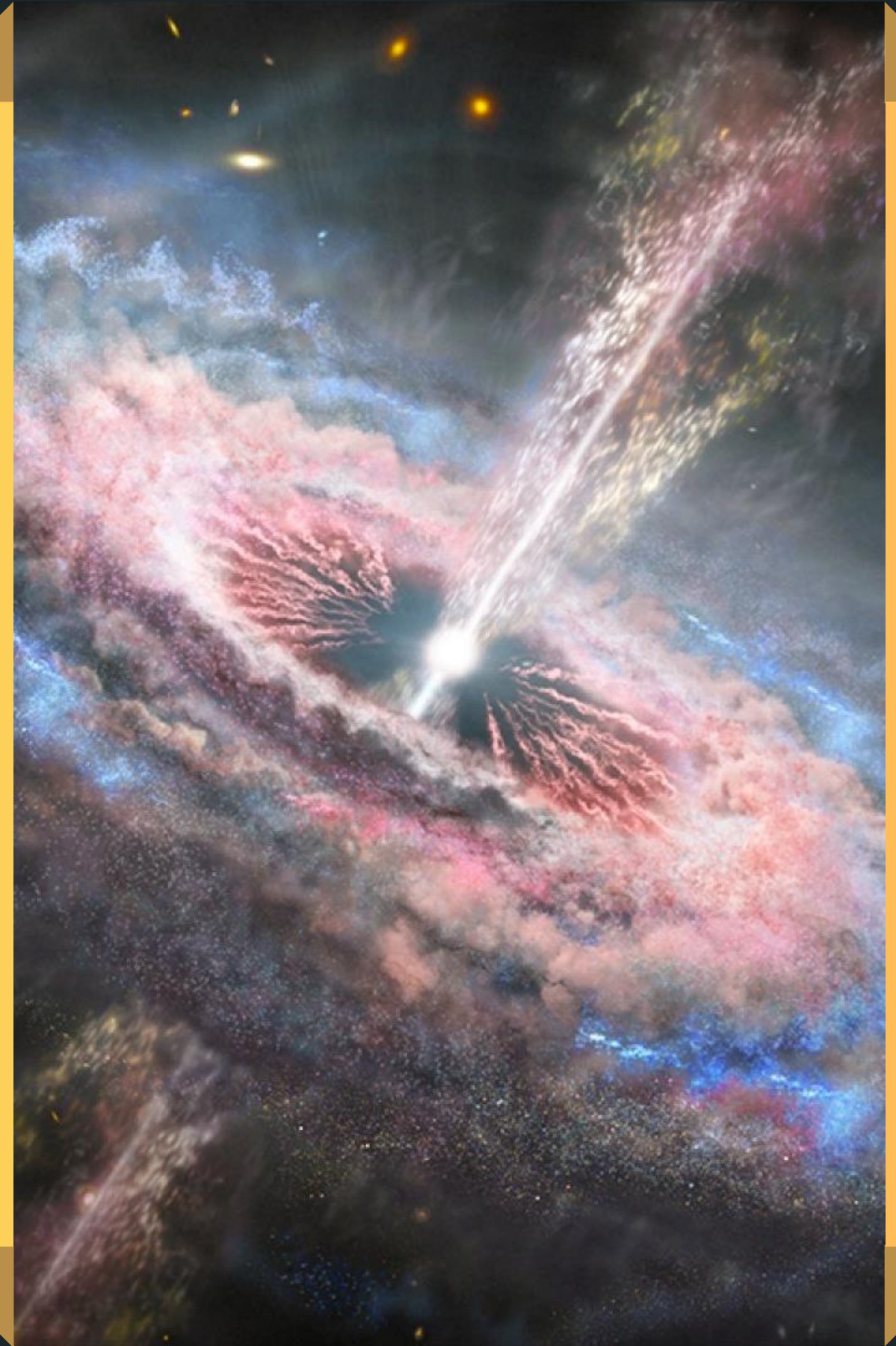
- Case of IceCube-170922A neutrino and the TXS 0506+056 blazar:
  - chance coincidence disfavoured at  $3\sigma$  significance level - scenario assuming a linear correlation between neutrino and  $\gamma$ -ray production or  $\gamma$ -ray flux variations.
- Detection of a single neutrino does not allow for the probing of details pertaining to neutrino production models, nor does it allow for the measurement of the neutrino-to- $\gamma$  production ratio.

# Summary

- There is a **wide variety of potential mechanisms** associated with the acceleration of particles to considerably superthermal energies within blazars.
- Current experimental efforts can **obtain the SED characterizing the photon emission blazars**. No such spectrum can be obtained for neutrinos thus far.
- Fits of models onto these spectra, namely in higher energy ranges, are likely to shed light on the relevance of the mechanisms mentioned, or even additional mechanisms.
- The case of TXS 0506+056 and the IceCube-170922A event, it is a crucial step towards a **definite association between blazars and neutrino emission**.

**THANK YOU  
FOR YOUR TIME!**

ANY QUESTIONS?



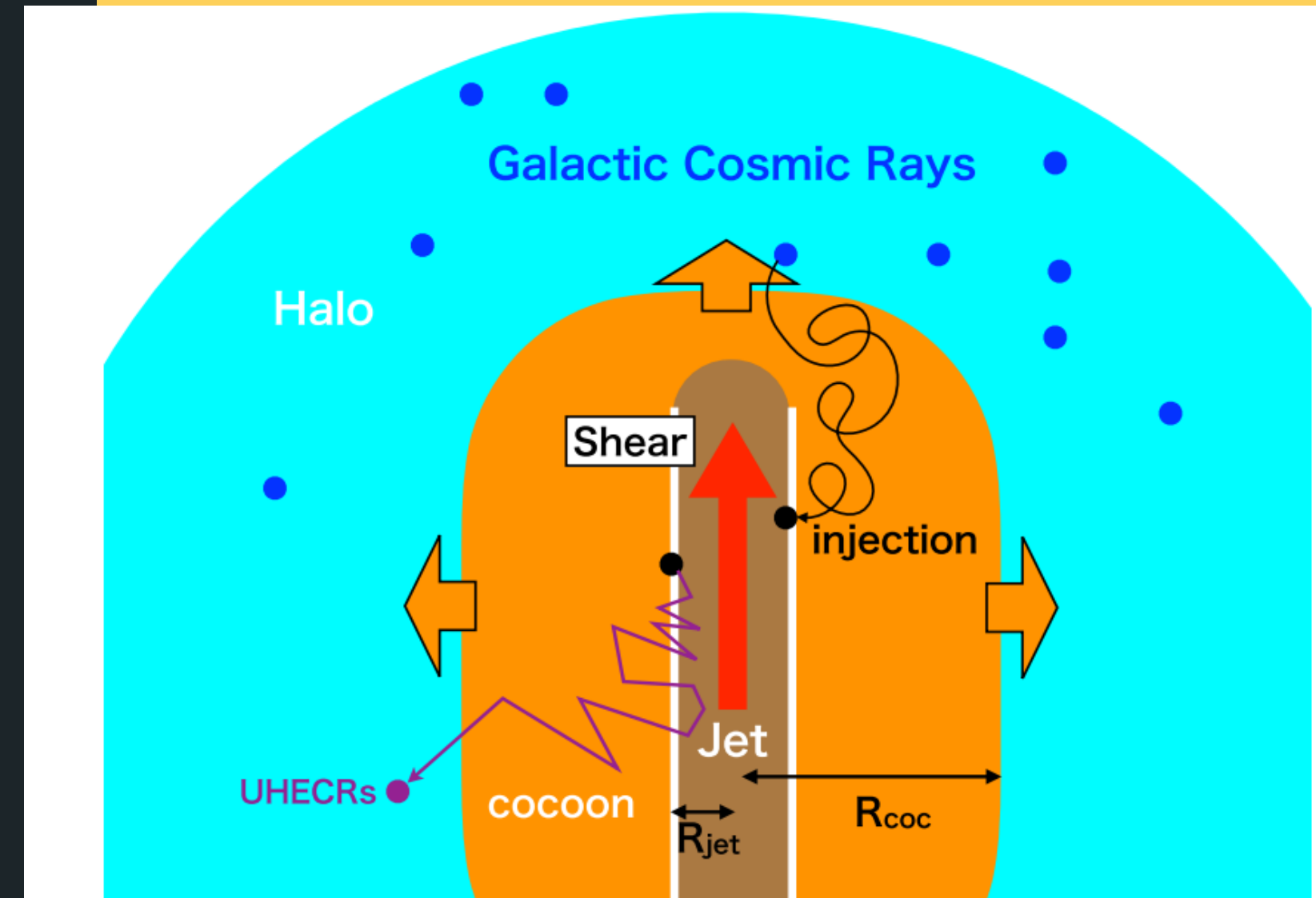
# OTHER MECHANISMS

## SHEAR ACCELERATION

Occurs when energetic particles encounter different local flow velocities as they are elastically scattered off small-scale magnetic field inhomogeneities.

## MAGNETIC KINK INSTABILITIES

Energy extracted via the development of hydromagnetic instabilities that act on the jet's helical magnetic field structure, the most relevant of which is the helical kink instability (KI).



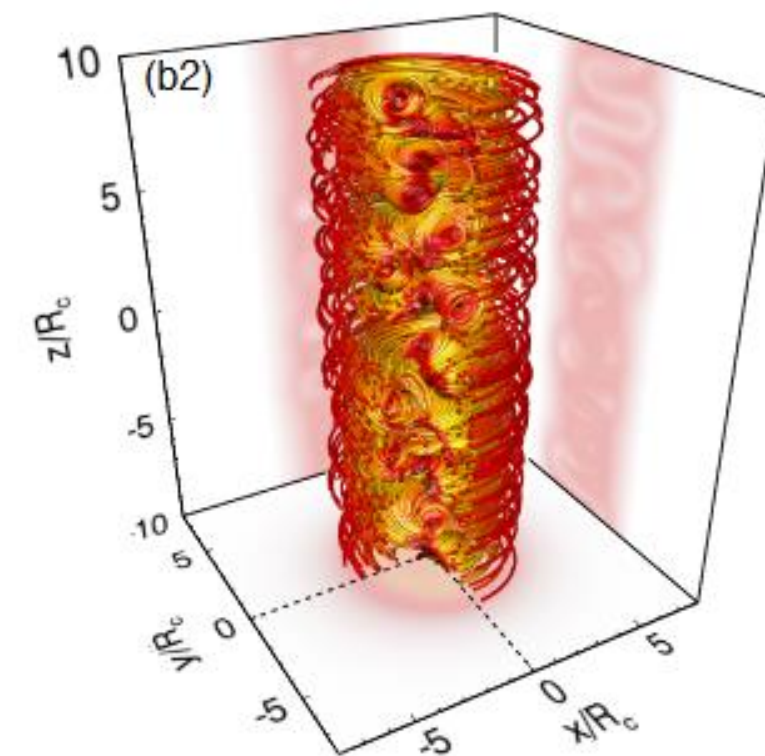
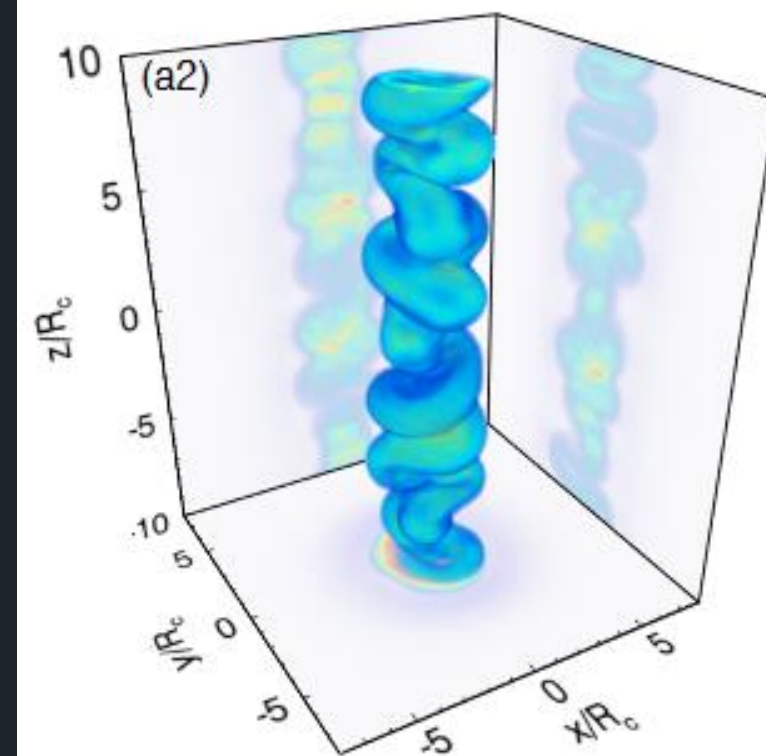
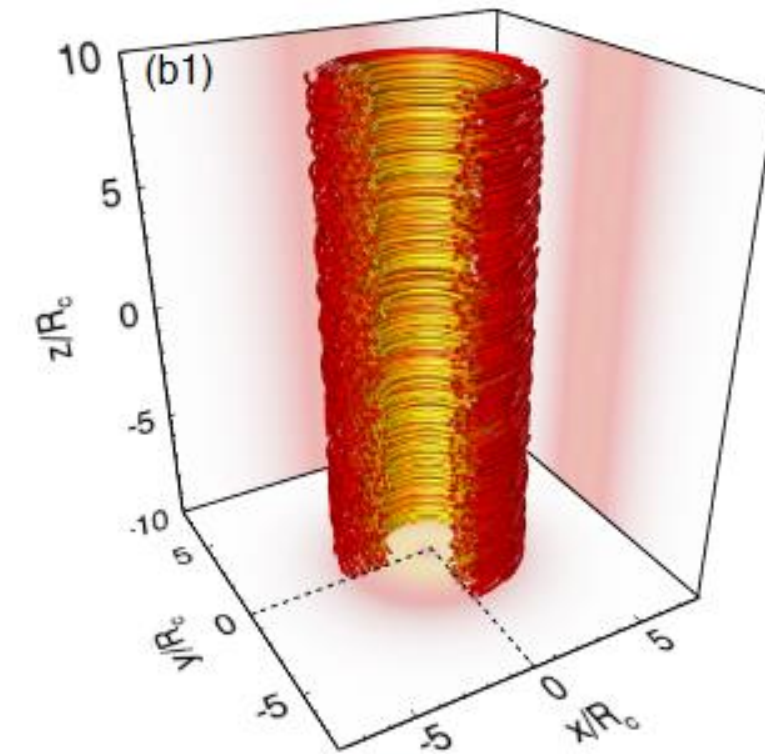
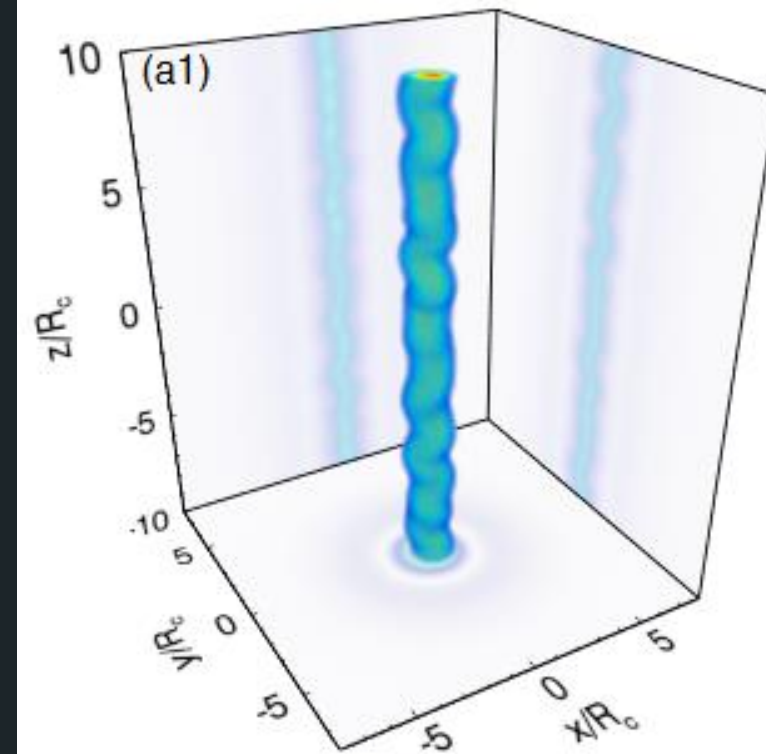
# OTHER MECHANISMS

## SHEAR ACCELERATION

Occurs when energetic particles encounter different local flow velocities as they are elastically scattered off small-scale magnetic field inhomogeneities.

## MAGNETIC KINK INSTABILITIES

Energy extracted via the development of hydromagnetic instabilities that act on the jet's helical magnetic field structure, the most relevant of which is the helical kink instability (KI).



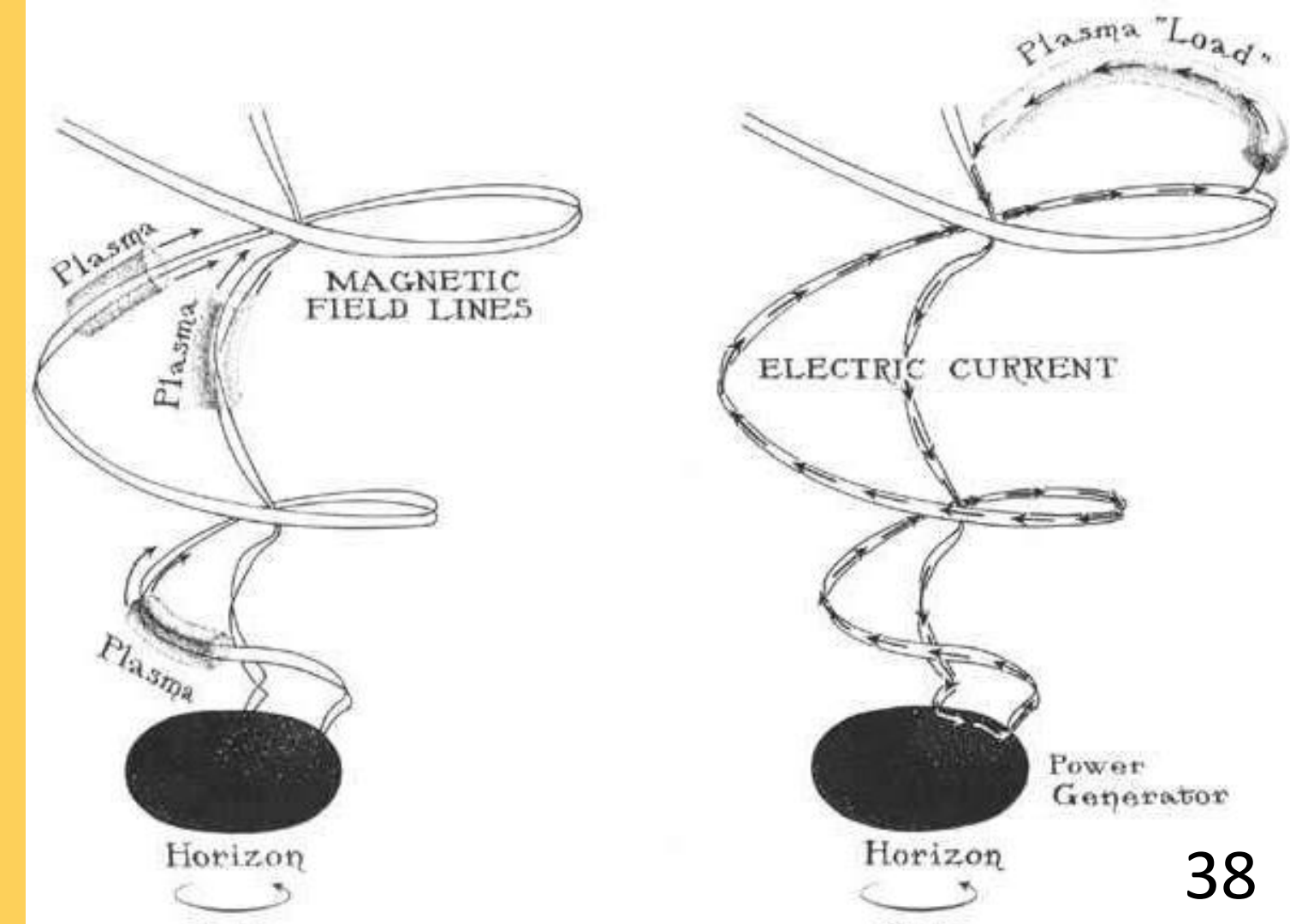
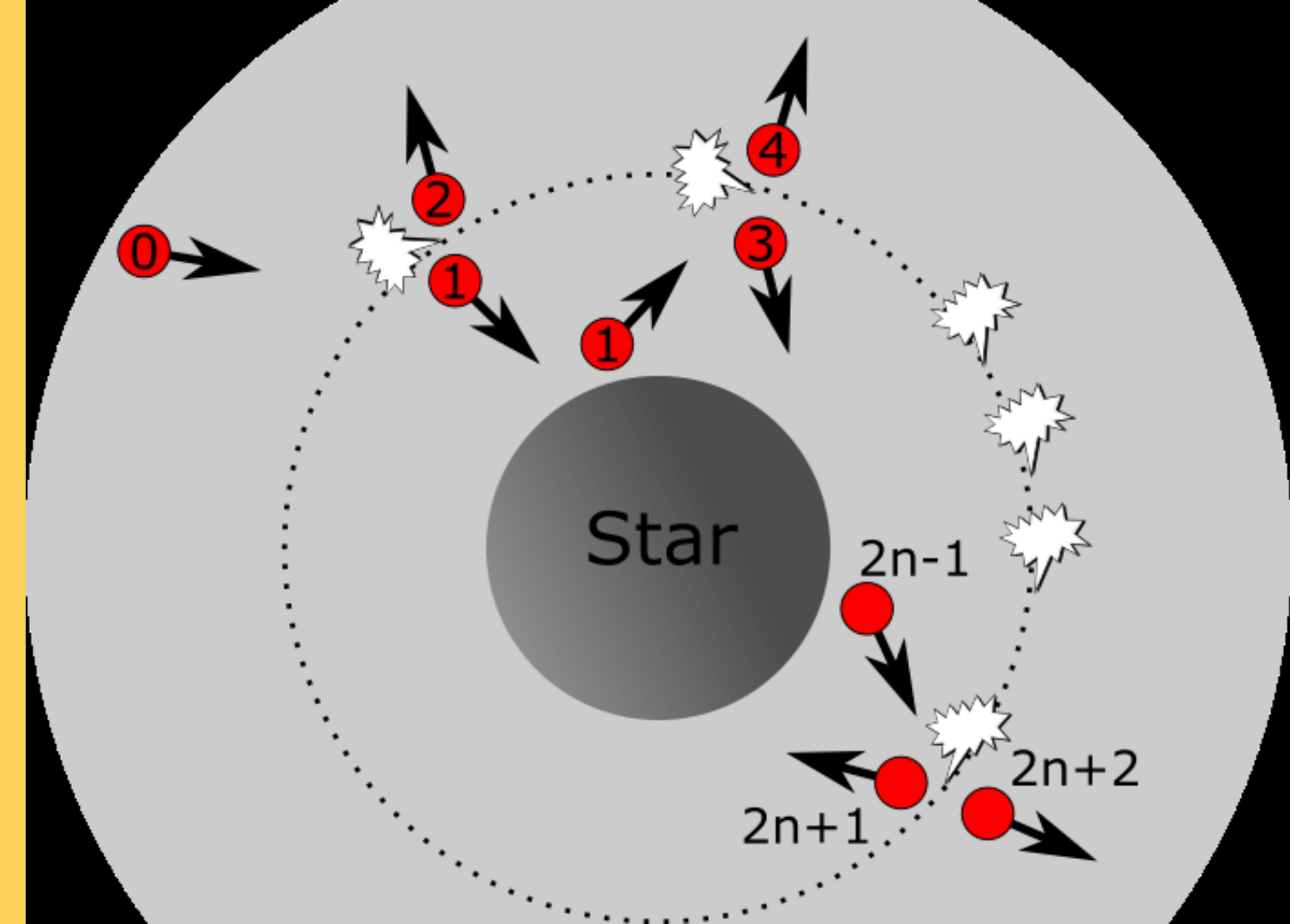
# OTHER MECHANISMS

## PENROSE PROCESS (PP) AND MAGNETIC PENROSE PROCESS (MPP)

Matter entering the ergosphere is split into two parts  
One escapes from the black hole, the other falls into it.  
Escaping particle can have greater mass-energy than  
the original piece of matter.

## BLANDFORD-ZNAJECK (BZ) MECHANISM

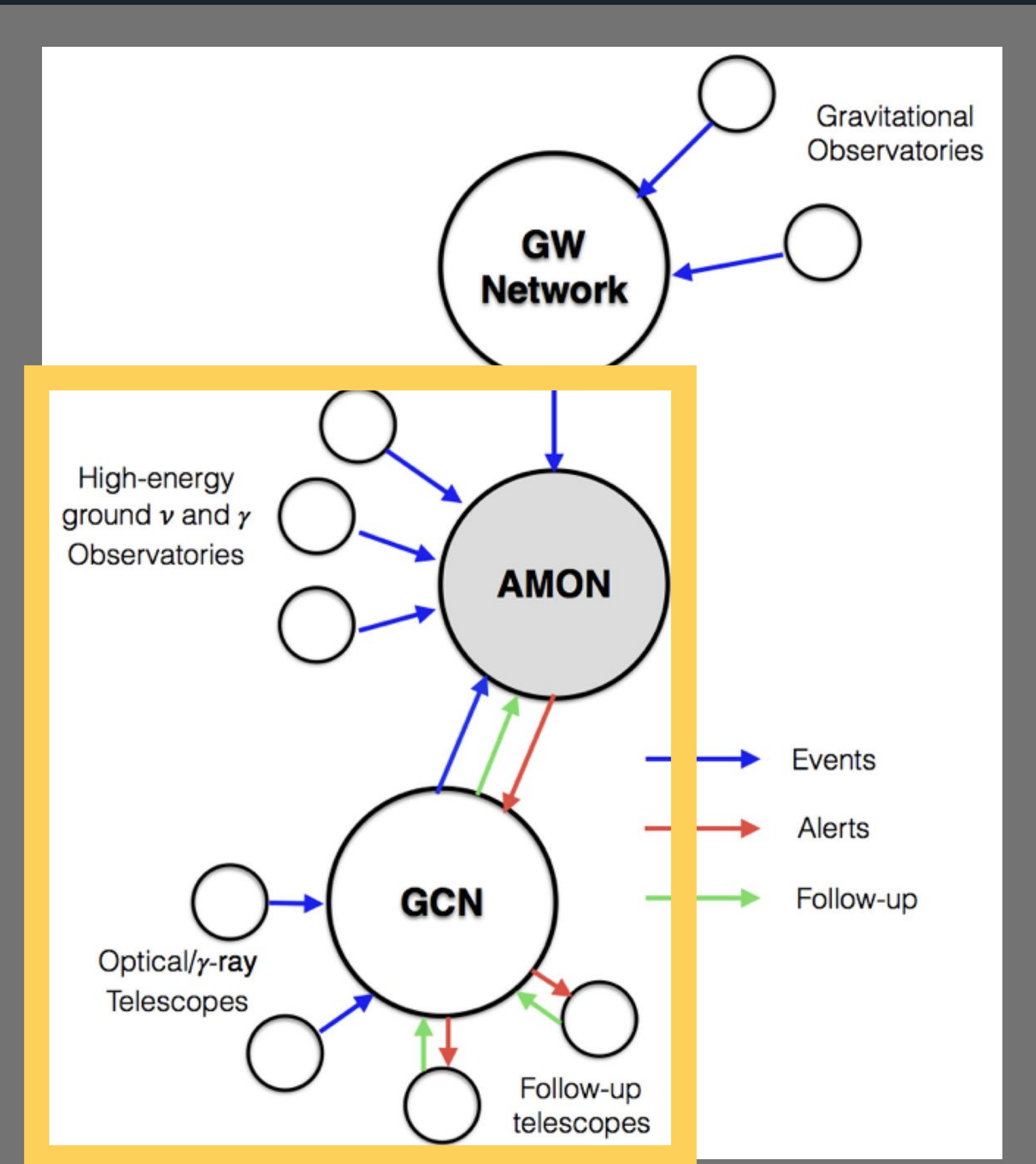
Ergosphere causes the magnetosphere inside it to  
rotate. Outgoing flux of angular momentum results in  
extraction of energy .



# ICECUBE ALERT SYSTEM

Alerts generated via the aforementioned systems are issued to the observational community through both public and private channels.

Public alerts make use of the Astrophysical Multimessenger Observatory Network (AMON) system as a gateway to the Gamma-ray Coordinates Network (GCN) and are immediately available to follow-up observatories.



# Models of blazar-neutrino flux correlation

**Model 1:** linear correlation between the neutrino energy flux and the  $\gamma$ -ray energy flux . Derived from the expectation that similar amounts of energy are channelled into neutrino and  $\gamma$ -ray emission, in the case that pion decays from pp or p $\gamma$  interactions are dominant at high energies.

**Model 2:** neutrino production and detection probability depends solely on the relative flux change of the  $\gamma$ -ray source. That is, neutrino flux is modelled as strongly correlated to variations in the observed  $\gamma$ -ray flux, regardless of its average value. This model implies that both weak or strong  $\gamma$ -ray sources are equally likely to be neutrino sources

**Model 3:** linear correlation between the neutrino energy flux and solely the VHE  $\gamma$ -ray energy flux .

# NEUTRINO-BLAZAR COINCIDENCE ANALYSIS

## LIKELIHOOD FUNCTION

S and B denote the signal and background probability density functions (PDFs), respectively. N is the total number of events and  $n_s$  is the number of signal events.

$$\mathcal{L} = \prod_i^N \left( \frac{n_s}{N} \mathcal{S} + \left(1 - \frac{n_s}{N}\right) \mathcal{B} \right)$$

$$TS = 2 \log \frac{\mathcal{L}(n_s = 1)}{\mathcal{L}(n_s = 0)} = 2 \log \frac{\mathcal{S}}{\mathcal{B}}$$

## TEST STATISTIC

Test between two fixed alternate hypothesis and allowing for the presence of negative values for background-like events.

